The Development of Techno-economic Models for Large-Scale Energy Storage Systems

Sahil Kapila, Abayomi Olufemi Oni, Amit Kumar[1]

University of Alberta, Department of Mechanical Engineering, 10-263 Donadeo Innovation Centre for Engineering, Edmonton, Alberta T6G 1H9, Canada

Abstract

The development of a cost structure for energy storage systems (ESS) has received limited attention. In this study, we developed data-intensive techno-economic models to assess the economic feasibility of ESS. The ESS here includes pump hydro storage (PHS) and compressed air energy storage (CAES). The costs were developed using data-intensive bottom-up models. Scale factors were developed for each component of the storage systems. The life cycle costs of energy storage were estimated for capacity ranges of 98-491 MW, 81-404 MW, and 60-298 MW for PHS, conventional CAES (C-CAES), and adiabatic CAES (A-CAES), respectively, to ensure a market-driven price can be achieved. For CAES systems, costs were developed for storage in salt caverns hard rock caverns, and porous formations. The results show that the annual life cycle storage cost is $220-400 for PHS, $215-265 for C-CAES, and $375-480 per kW-year for A-CAES. The levelised cost of electricity is $69-121 for PHS, $58-70 for C-CAES, and $96-121 per MWh for A-CAES. C-CAES is economically attractive at all capacities, PHS is economically attractive at higher capacities, and A-CAES is not attractive at all. The developed information is helpful in making investment decision related to large energy storage systems.

Keywords

Cost comparison; energy storage; large energy storage systems; compressed air energy storage; pumped hydro storage

Acronyms

[1]* Corresponding author. Tel.: +1-780-492-7797
E-mail address: Amit.Kumar@ualberta.ca (A. Kumar).

ALCC	Annual Levelized Capital Cost
A-CAES	Adiabatic Compressed Air Energy Storage
C-CAES	Conventional Compressed Air Energy Storage
CAES	Compressed air energy storage
ESS	Energy storage system
GHG	Greenhouse gases
KW	Kilowatt
KWh	Kilowatt hour
LCC	Life cycle cost
LCOE	Levelised cost of electricity
LCOS	Levelised cost of storage
NG	Natural gas
O&M	Operation and Maintenance
MW	Megawatt
MWh	Megawatt hour
PHS	Pumped hydro storage
SC	Storage cost
TEC	Total equipment cost
TIC	Total investment cost

1. Introduction

The use of fossils fuels to meet energy demands leads to greenhouse gas (GHG) emissions that cause environmental pollution and climate change [1-4]. The concerns of the public were recently addressed by reinforcing, in the Paris Agreement, the target to keep the global temperature increase well below 2°C above pre-industrial levels [5]. To achieve this target, there is the need for a reliable source of energy production that reduces GHG emissions, thereby improving the quality of the environment. Renewable sources of energy production such as wind and solar are widely recognized alternatives that will play a vital role in reducing GHG emissions [6, 7]. There has been a growth of more than 200% in the installed capacity of combined solar and wind energy production in recent years, from 183 GW in 2009 to 665 GW in 2014 [8]. Although these sources of renewable energy have many advantages, they also present some challenges [9]. They do not generate quantities of energy as large as those produced by traditional fossil fuels, and they are weather-dependent. Furthermore, they are intermittent, changing in intensity quickly as clouds pass over the sun or wind velocity changes [10]. The irregularity in wind and solar energy production leads to huge disruptions in electricity generation and poses challenges of load balance, grid stability, and reliability to energy network. Currently power and demand balance in the grid network is maintained by storing conventional fuels such as coal and natural gas. But wind and solar energy production demands additional flexibility in the system because of their sporadic nature [10, 11]. Energy storage systems can provide this flexibility and facilitate the integration of renewable energy sources in the grid network by storing energy at a time of surplus generation and releasing it at a time of deficiency [12]. These storage technologies can act as shock absorbers in the grid network and improve its efficiency, reliability, and security [13]. Thus, the introduction of an ESS in the energy network can address the aforementioned problem.

Energy storage is a vital link in the energy supply chain. In general, no more than 20% of an area's electricity demand can be met by renewables without the help of an ESS [14]. An ESS can lead to renewables' deployment in large quantities and thus is critical for a low carbon sustainable future. Lack of adequate information is a hindrance to the development of feasible business models for an EES. Although there are few ESSs around the world, they do not provide sufficient information on the economic sustainability of the systems. Therefore, it is imperative to conduct a comprehensive study that will provide more insight into the economics of an EES and develop the costs based on bottom-up approach.

Several studies address technical features such as the defining characteristics, system sizes, and applications of ESS [1, 9, 11, 12, 15-18]. However, the economic assessment remains obscure in most of the studies. Most of the studies provide information on the unit capacity capital cost (dollar per kW or dollar per kWh) without any detailed information on the development, life cycle cost and economic feasibility of ESS. The research by Schoenung et al. [19-21] on storage system costs use a top-down approach to estimate the benefits of storage technologies compared to costs for application categories such as bulk storage, distributed generation, and power quality. These studies, moreover, were limited to point estimates with the use of aggregated capital cost data. Data were collected from various suppliers and thus are generalized. Beaudin et al. [12] reviewed energy storage for mitigating renewables' variability and presented tabulated ranges of capital cost data based on earlier studies. No additional information was provided on equipment cost break-down, operating cost, etc. Akhil et al. [22] calculated the present worth and life cycle costs of discrete energy storage technology scenarios. Four scenarios were considered based on capacity and discharge time for Pumped Hydro Storage. The data were collected from suppliers and real life projects. However, that study's methodology lacks transparency and reproducibility. Viswanathan et al. [23] provided a qualitative and quantitative summary of capital cost and O&M cost data in existing literature. They provided a range of values rather than discrete numbers and estimated the future cost of an ESS. Bozzolani [24] did a detailed study on cost model development for Compressed Air Energy Storage. However, the study was limited to only this system and does not show its comparison with other large scale storage systems. Zakeri et al. [25] reviewed existing cost data and performed a comparative life cycle cost analysis of an ESS as well as an uncertainty analysis. Neither Bozzolani [24] nor Zakeri et al. [25] considered the economic viability of storage technologies or storage scale. The economy of scale is vital to determine the optimal plant size. Locatelli et al. [26] assessed the economics of large storage plants through a top-down methodology using capital investment data from the literature.

Most of these earlier studies used data from vendors or existing literature and used a top-down approach. They did not define system boundaries with respect to storage system capacity, develop bottom-up cost models, show economic assessment, nor report capital cost changes with changes in storage system capacity. In addition, there are wide variations and discrepancies in cost data since storage facility size and location are rarely considered in these analyses.

To address the aforementioned gap, the objective of this study is to develop data-intensive comprehensive techno-economic models for large energy storage systems. Pumped Hydro Storage (PHS) and Compressed Air Energy Storage (CAES) were considered in this study as they are prime candidates for large-scale storage application [27]. A detailed economic analysis was performed to investigate the economic feasibility of both systems in Alberta's (a province in Western Canada) electricity market. The specific objectives of the study are to:

1. Develop and model scenarios for PHS and CAES of different storage facility sizes.
2. Use a bottom-up methodology with the help of equipment cost relations to calculate the capital cost of a storage plant.
3. Assess the total investment required to build a storage plant of a specific size and operating cost.
4. Develop economies of scale and scale factors for PHS and CAES.
5. Estimate the selling price of the electricity produced by ESS in order to recover capital investment.
6. Conduct sensitivity and uncertainty analyses to identify important inputs.

The study will enable investors and policy makers to make informed decisions on investments and future policies for PHS and CAES.

2. Process description

2.1. Pumped Hydro Storage

PHS is a method of storing and generating electricity using two water reservoirs at different elevations. Presently, it is the most mature and commercially available technology and has more than 99% of installed ESS capacity [28, 29]. Figure 1 is a schematic diagram of a pump hydro system. The key components of a PHS plant are the pump turbine, motor, generator, penstock, inlet valve, penstock valve, upper reservoir, and lower reservoir. When the demand for electricity is low, the water in the lower reservoir is pumped to the upper reservoir. When the demand for electricity is high, the water from the upper reservoir flows to the lower reservoir, initiating the turbine to generate electricity. Two system valves regulate the flow of the water. The surge chamber facilitates the changes in water pressure.

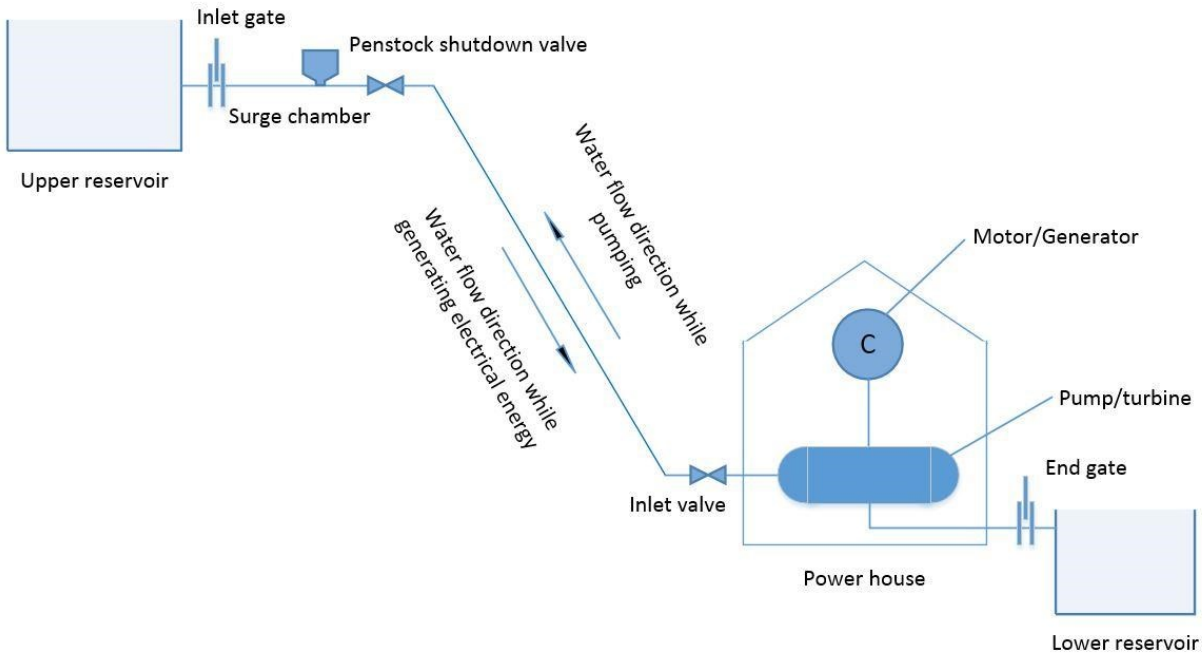

Figure 1: Pumped hydro storage schematic

2.2. Compressed Air Energy Storage

CAES is a method of storing electricity in the form of the potential energy of compressed air. It is the second commercially proven technology with a worldwide installed capacity of 440 MW [15]. CAES systems are of two types: conventional compressed air energy storage (C-CAES) and adiabatic compressed air energy storage (A-CAES).

2.2.1. Conventional Compressed Air Energy Storage

The main components of a C-CAES plant are the compressor, intercooler, valve, underground storage, recuperator, and turbine. Figure 2 presents a schematic of a conventional CAES system. During a period of low power demand, the excess electricity is supplied to compressors 1 to 3 to compress the air and convert electrical energy into potential air energy. The compressed air is then stored in an underground cavern, i.e., a salt cavern, porous formation, or hard rock cavern. During periods of high power demand, the air is supplied with energy by burning natural gas in combustors 1 and 2 and released through turbines 1 and 2 to produce electricity. The recuperator is installed just before the combustor to pre-heat the air with energy from exhaust gases and thereby increase overall system efficiency. The valves at the inlet and

outlet of the underground storage maintain constant pressure. Constant pressure ensures the turbines are operating at optimum points all the time, resulting in a more efficient system.

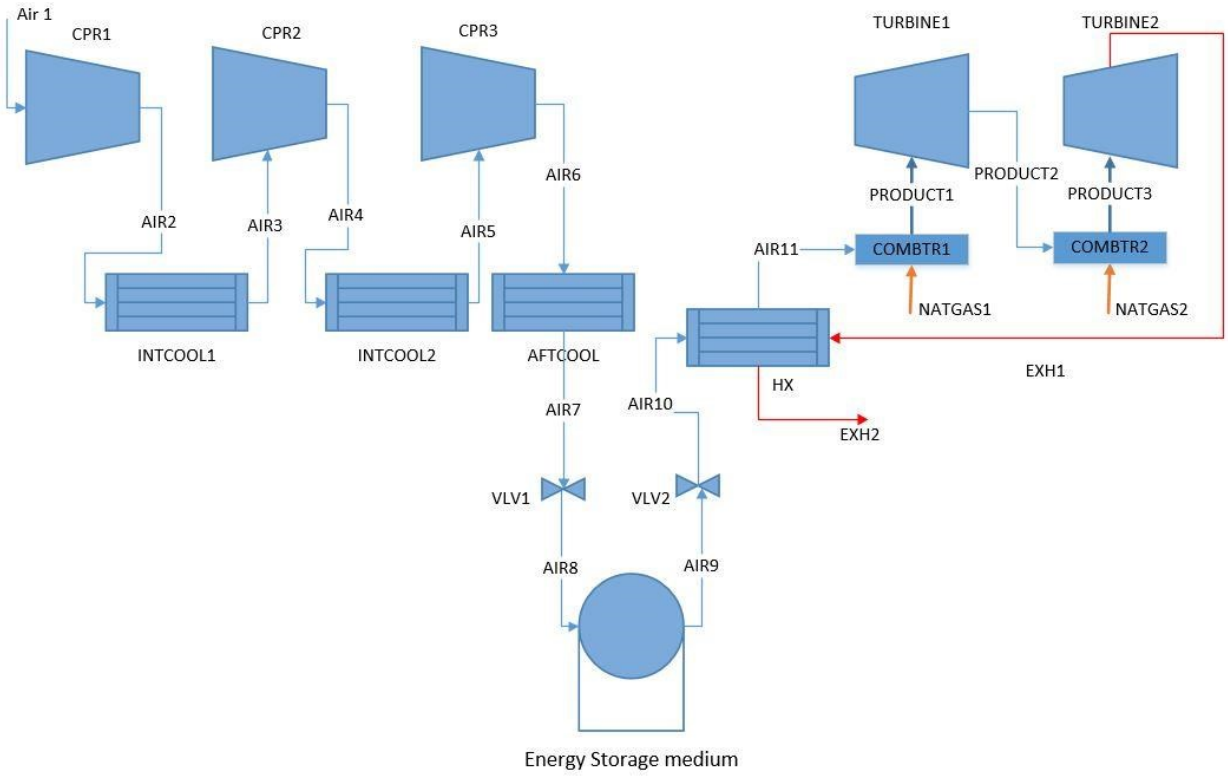

Figure 2: Conventional compressed air energy storage schematic

2.2.2. Adiabatic Compressed Air Energy Storage

The A-CAES system is the integration of CAES and a thermal energy storage system. The main components of the A-CAES system are the compressor, heat exchanger, underground storage, heat storage fluid, and turbine. Figure 3 is a schematic of the adiabatic CAES system. As for C-CAES, during periods of low power demand, excess electricity is supplied to compressors 1 and 2 to compress the air. The heat generated during compression is extracted from the compressed air with heat exchangers 1 and 2 and stored in working thermal fluid. The working fluid can be hot oil or a molten salt solution [26]. The compressed air is stored in an underground cavern. During periods of high power demand, the stored heat is recalled to heat the compressed air and then the air is released through turbines 1 and 2 to produce electricity. The heat storage powers the turbine to run without any help of fuel or gas.

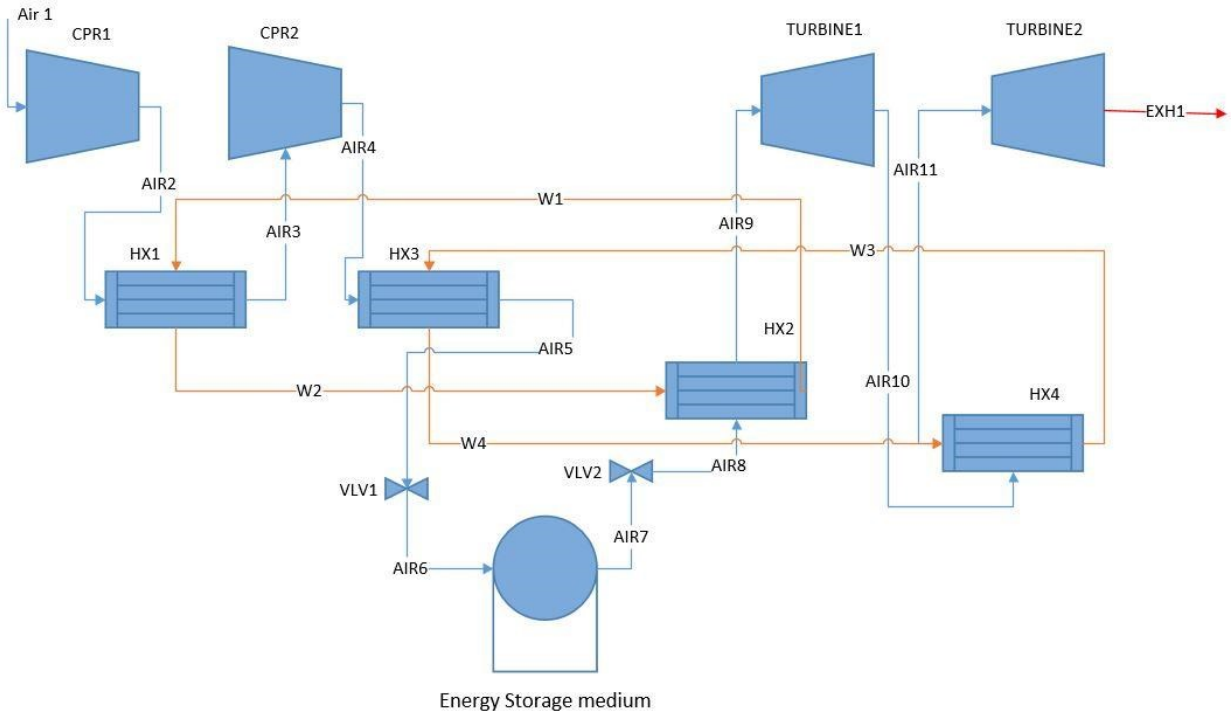

Figure 3: Adiabatic compressed air energy storage schematic

3. Model Development

3.1. Pumped Hydro Storage

The available head and the flow rate of water through the turbine are the essential input parameters in defining the power output from the PHS facility. As the head and flow rate increase, the power output of the PHS plant increases. The power output (□) is directly proportional to the head (□) and the flow rate (□), as defined in equation 1. The head is the available height differential of the reservoirs. The flow rate will depend on the size of the penstock. The energy output (□) of the PHS plant is directly proportional to the amount of water stored in the reservoir (□). The energy output of the PHS plant is calculated by equation 2. Generally, one cubic meter of water falling from a height of 100 m has the potential to produce 0.272 kWh of electricity [15].

$$□ = □ * □ * □ * □ * □ \quad (1)$$

$$□ = \frac{□_{□} * □ * □ * □ * □}{3.6 * 10^{9}} \quad (2)$$

Where □ is the overall efficiency of a PHS plant, □□ is the efficiency of PHS in generation mode, □ is the mass density of water (1000 kg/m^3), and □ is the acceleration due to gravity (m/s^2).

The output electrical energy from PHS was modeled using the parameters presented in Table 1. The data available from various operating PHS plants in the U.S were compiled [30, 31]. The important input parameters of a PHS plant were selected from the compiled data. The head and flow rate of a PHS plant base case were taken as 500 m and 60 m^3/s, respectively. The efficiency of the pump turbine is an important defining characteristic of a PHS plant as the power output depends on it. The efficiency of the pump turbine both in pumping and generation mode was taken as 0.9 [30]. Losses due to evaporation and frictional losses in penstock are negligible compared to losses in components [15] and thus were not included in the technical analysis. The PHS base case was modeled for a capacity of 294 MW. The developed PHS model is flexible enough to handle different plant capacities depending on unit operations. Scenarios of different plant capacities were created by varying input parameters.

Table 1: Input parameters for the pumped hydro storage model

Component	Type	Parameters	Value	Units	Reference
		Head	500	m	[31]
Pump turbine	Francis	efficiency (pumping)	0.9		[32]
		efficiency (Generation)	0.9		[32]
		No of units	1		
		Flow rate	60	m^3/s	[31]
		Velocity of flow	5	m/s	[31]
		Hours of operation (pumping)	8	hr	
Upper Dam	Concrete Dam	Dam height	35	m	Assumed
		Dam width	80	m	Assumed
Lower Dam)	Concrete Dam	dam height	25	m	Assumed
		Dam width	60	m	Assumed
Surge chamber		Height	100	m	Assumed

3.2. Compressed Air Energy Storage

The individual components of a CAES plant were modeled separately. The model used in this study was based on engineering thermodynamics equations.

The efficiency of the compressor (η_c) was calculated using equation 3 [33]. The outlet temperature of the compressor ($T_{out,comp}$) was determined using the ideal gas polytropic relation. The relation is presented in equation 4 [34, 35]. The required compressor power (P_{comp}) can be estimated based on air mass flow rate ($\dot{m}_{air}$) and the temperature difference across the compressor, as shown in equation 5.

$$\eta_c = 0.91 - \frac{r_c - 1}{300} \tag{3}$$

$$T_{out,comp} - T_{in,comp} = T_{in,comp} * (r_c^{\frac{\gamma-1}{\gamma*\eta_c}} - 1) \tag{4}$$

$$P_{comp} = C_{p,air} * \dot{m}_{air} * (T_{out,comp} - T_{in,comp}) \tag{5}$$

Where, r_c is the compressor pressure ratio and γ is the specific heat ratio of air.

The specific heat of air ($C_{p,air}$) was evaluated at an average compressor temperature using the relationship presented by McDonald and Magande [43]:

$$C_{p,air} = \frac{(28.11+0.1967*10^{-2}*T+0.4802*10^{-5}*T^2-1.966*10^{-9}*T^3)}{28.97} \tag{6}$$

where, T is the temperature difference across the equipment.

The pressure drop (P) through the intercooler is a function of heat exchanger effectiveness (ε) and inlet pressure (P_{in}) and was calculated using equation 7 [33]. The rate of heat exchange ($\dot{Q}$) through the intercooler or recuperator was calculated using equation 8 [38, 44]. The area of intercooler or after-cooler (A) required was calculated with the heat balance equation (9):

$$P = 0.0083 * \frac{\varepsilon}{1-\varepsilon} * P_{in} \tag{7}$$

$$\dot{Q} = U * (\dot{m} * C_p)_{min} * (T_{hot,in} - T_{cold,in}) \quad (8)$$

$$A = \frac{\dot{m}_{min} * C_{p,min} * NTU}{U * LMTD} \quad (9)$$

where $T_{hot,in}$ is the inlet temperature of the hot stream, $T_{cold,in}$ is the inlet temperature of the cold stream, U is overall heat transfer coefficient, and $LMTD$ is logarithmic mean temperature difference.

The cavern volume (V_c) required to store the air was calculated by equation 10:

$$V_c = \frac{R * T * \dot{m}_{air} * T_{storage}}{\frac{P_2}{P_1}} \quad (10)$$

where R is the specific gas constant taken, $T_{storage}$ is temperature of the storage cavern, and $\frac{P_2}{P_1}$ is the pressure differential required to fill the cavern.

The flow rate of natural gas ($\dot{m}_{NG}$) required in the combustor was measured using equation 11:

$$\dot{m}_{NG} = \frac{\dot{m}_{air} * C_{p,air} * \Delta T}{HV} \quad (11)$$

where HV is heating value of natural gas (KJ/kg).

The efficiency of the turbine (η_t) was evaluated using equation 12 [41]. The outlet temperature of the turbine ($T_{turbine.out}$) was also determined using the ideal gas polytropic relation. The relation is presented in equation 13 [34, 36]. The power delivered by the turbine ($P_{turbine}$) was calculated by equation 14.

$$\eta_t = 0.9 - \frac{r_p - 1}{250} \quad (12)$$

$$T_{turbine.out} = T_{in,turbine} - \eta_t * T_{in,turbine} * \left(1 - r_p^{\frac{\eta_t * (1-\gamma)}{\gamma}}\right) \quad (13)$$

$$P_{turbine} = \eta_t * \dot{m}_{air} * (T_{in} - T_{out}) \quad (14)$$

Five scenarios of different power output capacities were developed for both conventional and adiabatic CAES by varying unit operations. The flow rate was varied along with all linked parameters to accommodate the change in flow rate such as compressor power, storage cavern volume, amount of natural gas or heat storage fluid required, area of recuperator or heat exchanger, etc.

3.2.1. Conventional Compressed Air Energy Storage

The energy output from C-CAES was modeled using the parameters presented in Table 2. The air enters the system at 15°C and 1 bar of pressure. The air flow rate for the CAES base case was taken to be 300 kg/s. The compressed air is stored in an underground cavern at a pressure in the range of 45-70 bars [37]. To reach this pressure range, the system has three compressors each with a compressor ratio of 4.3. The effectiveness of intercoolers was taken to be 0.8 [38]. Two turbine systems were used to generate electrical energy, a high-pressure and a low-pressure turbine, with discharge pressures of 10 bars and 1 bar, respectively. The C-CAES plant base case was modeled for a capacity of 242 MW.

Table 2: Input parameters for the conventional compressed air energy storage model

Stream/Component	Parameter	Value	Units	Reference
Air	Inlet temperature	288.15	K	
	Pressure	1	bar	
	Flow rate	300	kg/s	
	Specific heat ratio	1.4		[39]
	Specific gas constant	287	J/kg K	[40]
Natural gas 1	Inlet temperature	288.15	K	
	Pressure	1	bar	
Natural gas 2	Inlet temperature	288.15	K	
	Pressure	1	bar	
	Lower heating value	48120	KJ/kg	[41]
Compressor 1	Compression ratio	4.3		[24]
Compressor 2	Compression ratio	4.3		[24]
Compressor 3	Compression ratio	4.3		[24]

Intercooler 1	Effectiveness	0.8		[38]
Intercooler 2	Effectiveness	0.8		[38]
	U value (Air to Water)	200	W/(m^{2}K)	[42, 43]
Aftercooler	Effectiveness	0.8		[38]
Storage Cavern	Inlet pressure	70	bar	[37]
	Outlet pressure	45	bar	[37]
	Temperature	303.15	K	
Recuperator	Effectiveness	0.8		[38]
	U value (Air to Air)	150	W/(m^{2}K)	[42, 43]
Combustor 1	Operating temperature	823.15	K	[44]
		1098.1		
Combustor 2	Operating temperature	5	K	[44]
	Turbine discharge			
Turbine 1	pressure	10	bar	[44]
	Turbine discharge			
Turbine 2	pressure	1	bar	[44]

3.2.2. Adiabatic Compressed Air Energy Storage

The energy output from A-CAES was modeled using the parameters listed in Table 3. The air enters the system at 15°C and one bar of pressure. The airflow rate for the CAES base case was taken as 300 kg/s. The compressed air is stored in an underground cavern at a relatively high pressure of 140-160 bar. A two-compressor system is used with a compressor ratio of 13.1. The effectiveness of heat exchangers was taken to be 0.9 [38]. Two turbine systems, high-pressure turbine and low-pressure, are used to generate electrical energy with discharge pressures of 15 bars and 1 bar, respectively. The discharge pressure of the high-pressure turbine was selected based on optimizing the total electrical output for the system. The A-CAES plant base case was modeled for a capacity of 179 MW.

Table 3: Input parameters for the adiabatic compressed air energy storage model

Stream/ Component	**Parameter**	**Value**	**Unit**	**Reference / Remark**
Air	Inlet temperature	288.15	K	

	Pressure	1	bar	
	Flow rate	300	kg/s	
	Specific heat ratio	1.4		[39]
Dowtherm T 1	flow rate (kg/s)	120	kg/s	
		288.1		
	Initial Temperature	5	K	
Dowtherm T 2	flow rate (kg/s)	120	kg/s	
		288.1		
	Initial Temperature	5	K	
Storage Tank 1	Number of Units	3		Assumed
Storage Tank 2	Number of Units	3		Assumed
Pump	Efficiency	0.7		[45]
	Head	20	m	Assumed
Compressor 1	Compression ratio	13.1		
Compressor 2	Compression ratio	13.1		
Heat exchanger 1	Effectiveness	0.9		[38]
Heat exchanger 2	Effectiveness	0.9		[38]
Heat exchanger 3	Effectiveness	0.9		[38]
Heat exchanger 4	Effectiveness	0.9		[38]
	U value	200	$W/(m^2K)$	[42, 46]
Storage Cavern	Inlet pressure	160	bar	[47]
	Outlet pressure	140	bar	[47]
		298.1		
	Temperature	5	K	
Turbine 1	Turbine discharge pressure	15	bar	[47]
Turbine 2	Turbine discharge pressure	1	bar	

4. Development of Techno-economic Models

4.1. Evaluation of Total Equipment Cost

The total equipment cost (TEC) is the sum of the cost of individual equipment required for the energy storage system. It comprises the power-related costs including the purchase and installation costs of all the power equipment in the storage system. Individual equipment costs were calculated using the cost functions of equipment found in the literature [48-50]. A list of

equipment for PHS and CAES and their cost functions is presented in Supplementary Section (Appendix A)[2]. These cost functions are adjusted to incorporate location factor and exchange rate.

4.2. Evaluation of Storage Cost

The storage cost (SC) evaluates the energy-related costs for the storage systems including the construction cost of reservoirs for PHS and the underground air storage reservoir for CAES.

For PHS, the reservoir cost (C_r) is calculated through an equation from Dawes and Wathne [51].

$$C_r = 5.5663 * (196.22 * V_r^{0.54} + 0.001 * V_r^{0.87} * L) \quad (15)$$

Where V_r is the reservoir volume and L is the land unit cost ($ per acre).

The land unit cost was taken to be $10,000 per acre [52]. This figure is based on the upper range of land cost in Alberta and was selected in order to have conservative estimates.

Three CAES storage media were considered in this analysis: salt, porous formation, and hard rock cavern. The cost of each was calculated based on construction materials. For a salt cavern, the total storage cost was broken down into four components: drilling, piping, water supply, and labor cost. For porous formations, drilling, piping, and labor costs were considered. The drilling depth (D) required for both salt caverns and porous formations was taken as 800 m based on existing CAES plants [53]. The per meter drilling cost was taken as $150/foot [54]. Steel was selected as the material for the construction of air channels. The piping cost was calculated based on the mean diameter of piping and pipe length. The mean diameter of the pipe (d) was taken as 20 inches [53]. The piping cost (C_{pipe}) was calculated as follows [50]:

$$C_{pipe} = 1.3129 * d^{1.1052} * D \quad (16)$$

About fifty gallons of water are required per cavern unit volume [52]. Water is available free of charge as it is assumed that there is an unlimited source of water nearby like a river or lake. But this water needs to be transported to the cavern site. Thus, transportation costs will be incurred. The average distance between the water source and the cavern is assumed to be 2 km. Pipes

[2] All costs are in 2014 U.S. dollars

and pumps are required to transport the water, and electricity is needed to operate the pumps. For the construction of the cavern, the labor cost was calculated assuming 10 laborers working for $35/hour [55]. It normally takes about two years to construct a salt cavern [37].

For hard rock formation, a limestone mine was considered. For underground mining, a room and pillar were selected for the creation of a hard rock cavern. Related costs were derived from Denholm and Kulcinski [27]. The construction time was taken as 300 days, and a 50% capital recovery factor was assumed. In addition, the gains from limestone are assumed to contribute one-third of the investment and operation cost.

4.3. Calculation of Total investment cost

The total investment cost (TIC) includes all power- and energy-related costs, and the balance of plant. This cost indicates the amount required upfront to build the storage facility. The TIC is derived from the total equipment cost following the methodology shown in Figure 4 [48, 56]. The method used is a standard method present in existing literature and generally acceptable for new plant construction. The TIC has four components: total direct cost, indirect cost, contingency, and storage cost. The total direct cost is further divided into the sub-components equipment cost, an additional 5% for accounted components, building, site development, and initial working capital. The indirect cost includes the contractor fee owner and insurance. The contingency is taken to be 10% of the total direct cost, while decommissioning cost is assumed to be zero [57] . The cost of the power conditioning system (PCS), which facilitates the integration of the plant to the grid, was not considered in the analysis.

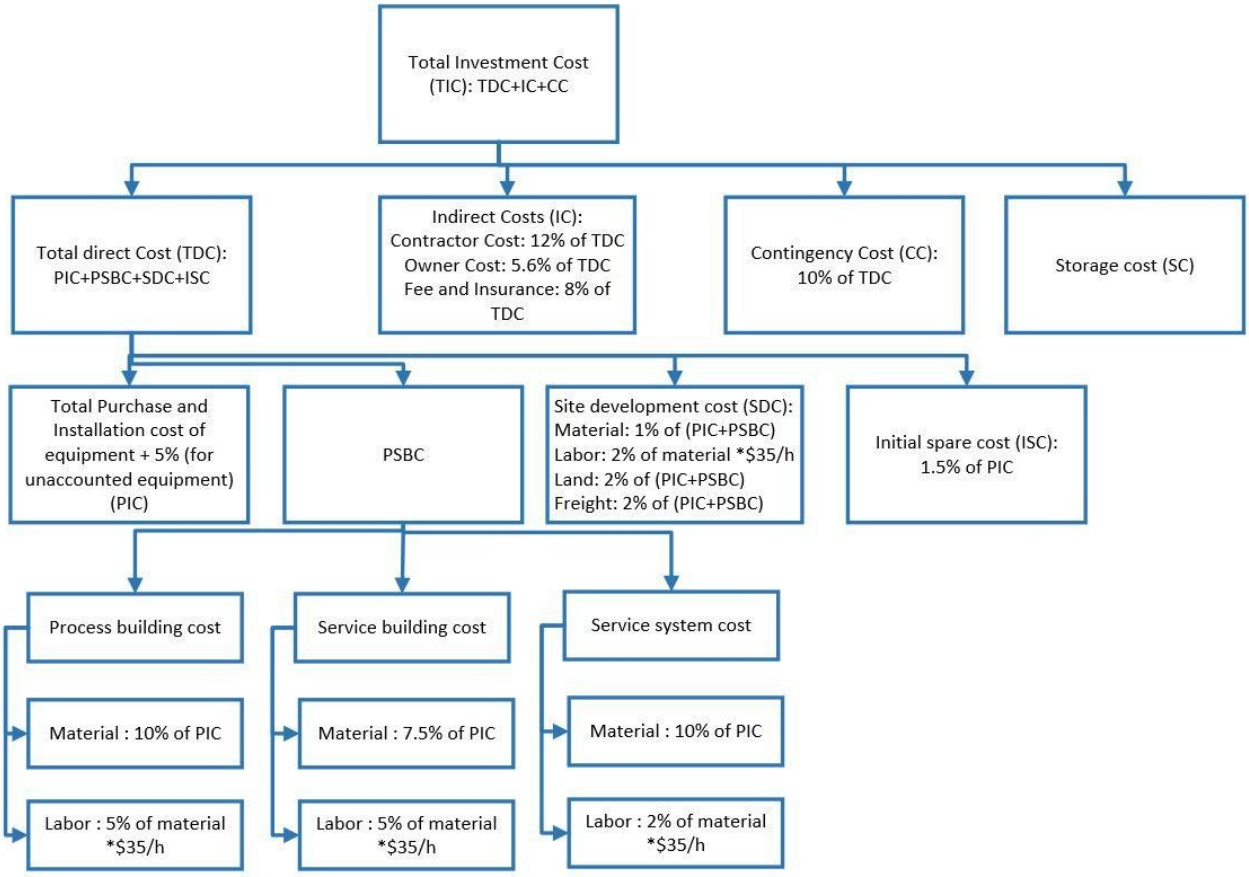

Figure 4: Methodology for the total investment cost calculation

4.4. Development of scale factor

The scale factor shows the effect of plant capacity on the TIC and defines the cost of one plant size relative to another. The scale factor [redacted] for an EES is determined by curve fitting the TIC to the plant capacity. It is defined through the following equation [49]:

[redacted] (17)

where [redacted] is the cost of the required plant, [redacted] is the base case plant cost, [redacted] is the capacity of the required plant, and [redacted] is the base case plant capacity.

4.5. Operation & Maintenance costs

For PHS, it is assumed that there are 20 employees working at an average salary of $65,000, which is incorporated in the operation and maintenance (O&M) cost. Other office supplies involve 10% of employee wages [58]. Annual maintenance and replacement costs are 2% of the TIC [59]. Overhaul cost is considered to be part of maintenance and replacement costs. The same methodology was used as for CAES to have uniformity and consistency in comparison.

4.6. Annual life cycle cost

The annual life cycle cost (□□□□) refers to the yearly payment to cover upfront costs and loan repayment if any [25] and is expressed in $/kW-year. The ALCC includes the TIC and O&M costs (including replacement costs) and annual fuel cost (electricity and other fuels such as natural gas). Both the TIC and O&M are annualized to calculate the ALCC. Before the ALCC is calculated, the capital recovery factor (□□□) needs to be defined. The capital recovery factor converts the total investment in annual installation over the life of the project based on the interest rate. The □□□ is calculated with equation 17. The interest rate (□) selected for the ALCC analysis is 10%. Once we have the CRF, the ALCC is calculated by equation 18.

$$□□□ = \frac{□ * (1 + □)^{□}}{(1 + □)^{□} - 1} \tag{18}$$

$$□□□□ = (□□□ * □□□ + □\&□ + □□□□_{□□□□□} * □ * □□□□_{□□□□□□□□□}) \tag{19}$$

where □ is the number of cycles in a year.

4.7. Levelised cost of electricity

The levelised cost of electricity (□□□□) is the price at which the electricity produced by an ESS should be sold at the given conditions to cover all the costs related to the ESS over its lifetime. The LCOE can be expressed in $/kWh or $/MWh. The plant life (□), number of operation cycles per year (□), and electricity input cost ($□□□_{□□□□□}$) are required to calculate the LCOE. The required assumptions to calculate the LCOE for both PHS and CAES are presented in Table 4. For the energy arbitrage application, the LCOE is compared with off-peak and on-peak electricity prices in Alberta. Alberta's electricity market is a deregulated market managed by the Alberta Electric System Operator. Electricity prices are set in real time. The dynamic of this market and high price fluctuation create ideal conditions for energy arbitrage [15]. The Alberta Electricity System Operator separates each day into two periods: on-peak and off-peak [60]. The on-peak period starts at 7:00 am and ends at 11:00 pm. The off-peak period is the

remaining eight hours. Electricity demand is higher during the on-peak period than the off-peak period and so are the electricity prices; thus, there is an opportunity for energy arbitrage. The average values of on-peak and off-peak electricity prices in Alberta over the last 10 years (2005-2014) were calculated [60]. It is assumed that storage facilities go through a full charge and a discharge cycle once a day, 350 days a year. A two-week maintenance period per year is assumed, and the plant is shut down during this time. The system charging time is 10 hours for both PHS and CAES plants. Both PHS and CAES are leaders on the storage technology maturity curve [10]. Though PHS has a few decades of early maturity over CAES, the equipment required for CAES is used in other developed industries such as conventional gas turbine plants. Thus, it is assumed that risk associated with both technologies is the same, and a discount rate of 10% is used for both technologies for consistency. A discount rate of 10% is within the range of values present in existing literature [20, 21, 25]. Furthermore, the impact of discount rate on the overall cost was also investigated by performing a sensitivity analysis.

Table 4: Data for the LCOE calculation

	PHS	**CAES**	**Reference**	**Comments**
Construction time (years)	7	2	[30, 37, 58]	
No. of cycles in a year	350	350		One cycle per day, two weeks for annual maintenance
Life (years)	50	40	[10, 12]	Average life based on different sources
Off-peak pool price ($/MWh)	28.18	28.18	[60]	Average calculated for years 2005-14
On-peak pool price ($/MWh)	77.84	77.84	[60]	Average calculated for years 2005-14
Discount rate (r)	10%	10%		Assumed
Average inflation (f)	2%	2%	[61]	Average rate of inflation in Canada

The LCOE was calculated as:

$$LCOE = \frac{\left(\frac{C}{\frac{1+r}{1+f} * \left(\left(\frac{1+r}{1+f}\right)^{n} - 1\right)} + O\&M + C_{charging} * n * E_{discharged}\right)}{\left(\frac{1+r}{1+f} - 1\right) * E_{discharged}} \quad (20)$$

where $E_{consumed}$ is the electricity consumed in one cycle and $E_{produced}$ is the electricity produced in one cycle.

4.8. Levelised Cost of Storage

The levelised cost of storage (LCOS) was derived by subtracting the system charging cost from the LCOE. The LCOS includes all the net internal costs except the cost of charging the system. The LCOS is calculated as:

$$LCOS = LCOE - \frac{Cost\ of\ charging\ the\ system}{Discharged\ electricity} \quad (21)$$

5. Results and discussion

5.1. Development of technical scenarios

5.1.1. Pumped Hydro Storage

The simulation results from five PHS scenarios are reported in Table 5. The scenarios were generated by varying the water flow rate in equally spaced intervals from 20 to 100 cubic meters. The plant's power capacity output in each scenario is 98, 196, 294, 392, and 491 MW. The energy output of one cycle for different scenarios ranges from 795 to 3973 MWh. As the water rate increases, the power input and energy output from the plant also increase. The water requirement ranges from 0.72 to 3.6 million cubic meters.

Table 5: Technical results for pumped hydro storage

		Scenarios				
	Parameter	**1**	**2**	**3**	**4**	**5**
Simulation Input	Water flow rate (m^3/s)	20	40	50	60	100
	Head (m)	500	500	500	500	500
Simulation Output	Water volume(thousand m^3)	720	1440	2160	2880	3600
	Power capacity (MW)	98	196	294	392	491
	Energy output in one cycle (MWh)	795	1589	2384	3178	3973

5.1.2. Compressed Air Energy Storage

5.1.2.1. Conventional Compressed Air Energy Storage

The simulation results from five C-CAES scenarios are reported in Table 6. These scenarios were generated by varying the air flow rate in equally spaced intervals from 100 to 500 cubic meters. The plant's power capacity output in each scenario is 81, 162, 242, 323, and 404 MW. The C-CAES plant's power output increases with an increase in air flow rate. The compressor efficiency is constant and is equal to 0.86 for all scenarios. The input power required by each compressor is also listed in Table 6. The minute difference in the power requirement by the three compressors is because they operate at different temperatures and the specific heat capacity of air changes slightly with temperature. The intercooler and the recuperator areas were also calculated and found to increase with an increase in power output. For any one scenario, the intercooler area required decreases from intercooler 1 to intercooler 3. This happens because of the increase in air pressure from intercooler 1 to intercooler 3. The total flow rate of natural gas varies from 2.03 to 10.15 kg/s. The efficiency of the high- and the low-pressure turbines is 0.90 and 0.89, respectively, and is the same for all scenarios. The individual output of each generator is included in the table.

Table 6: Simulation results for conventional compressed air energy storage

		Scenarios				
	Parameter	**1**	**2**	**3**	**4**	**5**
Simulation Input	Air flow rate (m^3/s)	100	200	300	400	500
	Compressor efficiency	0.86	0.86	0.86	0.86	0.86
	Compressor 1 power (MW)	17.25	34.50	51.75	69.01	86.26
	Compressor 2 power (MW)	17.57	35.14	52.71	70.28	87.85
	Compressor 3 power (MW)	17.89	35.78	53.66	71.55	89.44
	Intercooler 1 area (m^2)	2182	4365	6547	8730	8730
	Intercooler 2 area (m^2)	1757	3513	5270	7027	7027
	Intercooler 3 area (m^2)	1521	3042	4563	6084	6084
	Recuperator area (m^2)	2,362	4724	7085	9447	9447
	Natural gas flow rate (kg/s)	2.03	4.06	6.09	8.12	10.15
	Efficiency of turbine 1	0.9	0.9	0.9	0.9	0.9
	Efficiency of turbine 2	0.89	0.89	0.89	0.89	0.89
Simulation Output	Generator 1 Output (MW)	28	56	84	112	140
	Generator 2 Output (MW)	53	106	158	211	264
	Output capacity (MW)	81	162	242	323	404

5.1.2.2. Adiabatic Compressed Air Energy Storage

The simulation results from five A-CAES scenarios are reported in Table 7. The scenarios were generated by varying the air flow rate in equally spaced intervals from 100 to 500 cubic meters. The plant's power capacity output in each scenario is 60, 119, 179, 239, and 298 MW. The A-CAES base case has a capacity output of 179 MW. The A-CAES plant's power increases with an increase in air flow rate. The compressor efficiency is constant and is equal to 0.87 for all scenarios. The input power required by each compressor is also listed in Table 7. Here, the difference between the power requirements of compressor 1 and compressor 2 is significant because of the high variation in the operating temperature of the two compressors. The heat exchanger area was also calculated and found to increase with an increase in power output. For any given scenario, the area of heat exchangers 3 and 4 is less than that of heat exchangers 1 and 2 as heat exchangers 3 and 4 operate at higher pressure. The efficiency of the high- and the low-pressure turbines is 0.87 and 0.85 respectively and is same for all scenarios. The individual output of each generator is included in Table 7.

Table 7: Simulation results for adiabatic compressed air energy storage

		Scenarios				
	Parameter	**1**	**2**	**3**	**4**	**5**
Simulation Input	Air flow rate (m^3/s)	100	200	300	400	500
	efficiency of compressor	0.87	0.87	0.87	0.87	0.87
	Compressor 1 Power (MW)	39.69	79.39	119.08	158.78	198.47
	Compressor 2 Power (MW)	45.36	90.72	136.08	181.44	226.81
	Heat exchanger 1 Area (m^2)	5814	11627	17441	23254	29068
	Heat exchanger 2 Area (m^2)	8109	16218	24327	32435	40544
	Heat exchanger 3 Area (m^2)	4885	9771	14656	19542	24427
	Heat exchanger 4 Area (m^2)	3289	6577	9866	13154	16443
	efficiency of turbine 1	0.87	0.87	0.87	0.85	0.87
	efficiency of turbine 2	0.85	0.85	0.85	0.00	0.85
Simulation Output	Output of Generator 1 (MW)	26	52	79	105	131
	Output of Generator 2 (MW)	33	67	100	134	167

Output Capacity (MW)	60	119	179	239	298

5.1.3. Total Investment Cost and Scale factor

The total investment cost is comprised of power cost and energy cost. The power cost is the cost of the equipment that determines the plant's power capacity (i.e., the pump). The energy cost is simply storage cost and relates to the energy output capacity of the plant. The units of power cost and energy cost are dollar per kW and dollar per kWh of one cycle respectively.

The power and energy costs for different PHS scenarios are shown in Table 8. For each scenario, two energy cost sub-scenarios were created, one for two-reservoir and one for one reservoir. The PHS energy cost includes the reservoir construction cost. In the two-reservoir scenario, it is assumed that both reservoirs (lower and upper) need to be built. For the one reservoir scenario, it is assumed one of the reservoirs exists and only one needs to be built. The PHS power cost ($ per kW) is from $800 to $2000. The energy cost ($ per kWh) for the two-reservoir scenario is from $40 to $55 and for the one reservoir scenario, $20 to $27. Both the power cost and the energy cost decrease with an increase in plant capacity because of economies of scale. The TIC for the PHS ranges from 200 to 550 million, as shown in Figure 5. In addition, the plot of the total investment with respect to the storage plant's power capacity has a scale factor 0.52. This means that the investment cost increases at a much lower rate than the increase in storage plant power output capacity, thus ensuring a higher return on investment for plants of higher power capacities. The scale factor established a strong economy of scale for PHS, i.e., an increase in capacity drastically reduces unit capital cost.

Table 8: Power and energy costs and plant capacities for pumped hydro storage

Plant capacity (MW)	**Power cost ($/kW)**	**Energy cost ($/kWh)**	
		Two-reservoir	**One reservoir**
98	2005	55	27
196	1245	49	24
294	1039	45	23
392	894	43	22
491	801	42	21

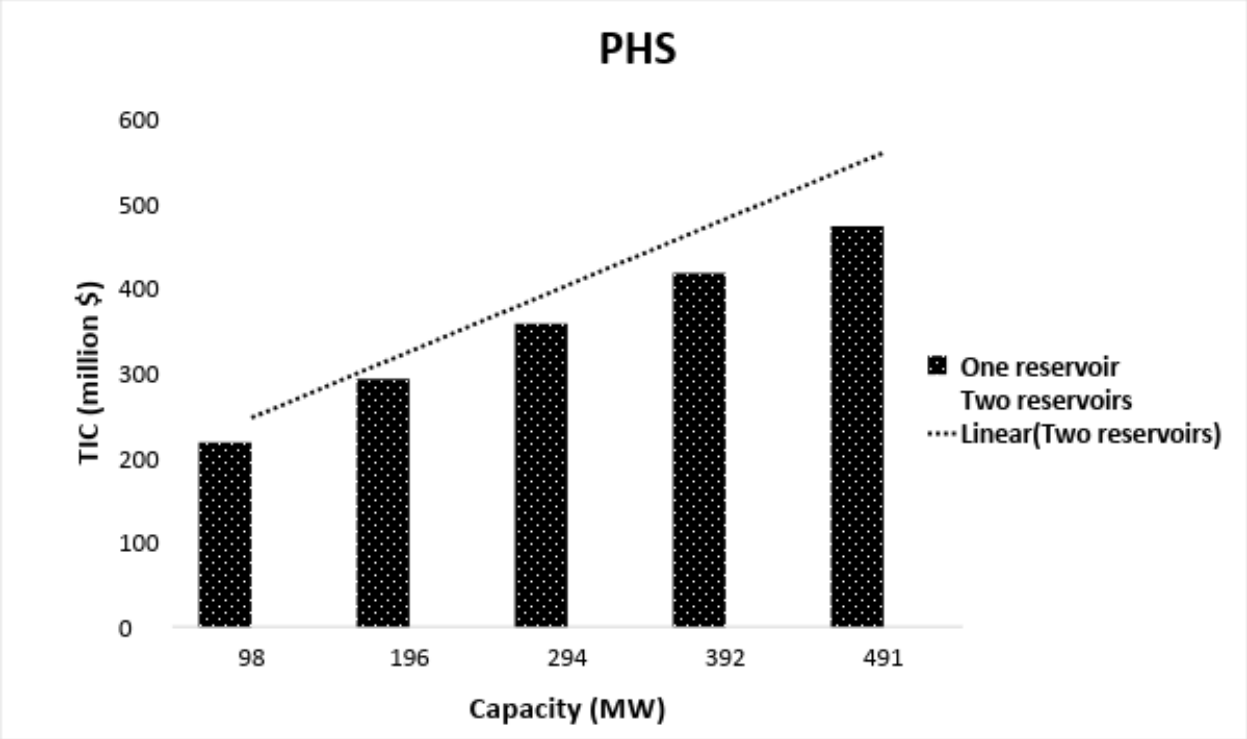

Figure 5: Total investment cost for pumped hydro storage

The power and energy costs for different C-CAES and A-CAES scenarios are presented in Table 9 and 10 respectively. The scenarios are divided into three categories depending on storage type (salt, porous formation, or hard rock cavern). For C-CAES, the power cost is in the range of $600 to $710/kW. Energy costs are in the range of $3 to $7/kWh for the salt cavern, $1 to $3/kWh for the porous formation, and around $30 for the hard rock formation. For A-CAES, the power cost is in the range of $1880 to $2230. Energy costs are in the range of $4 to $11/kWh for the salt cavern, $1 to $4/kWh for the porous formation, and around $50/kWh for the hard rock formation. The TIC for C-CAES and A-CAES ranges from 60 to 270 and 140 to 700 million, as shown in Figure 6 and Figure 7, respectively. In addition, the plot of the total investment with respect to the storage plant's power gives a scale factor of 0.87 for C-CAES and 0.88 for A-CAES. There are economies of scale established for C-CAES and A-CAES but they are not as strong as for PHS.

Table 9: Power and energy cost variations with plant capacity for conventional compressed air energy storage

Plant Capacity (MW)	Power cost ($/kW)	Energy cost ($/kWh)		
		Salt cavern	Porous formation	Hard rock cavern
81	707	7	3	30
162	657	5	1	30
242	633	4	1	30
323	619	3	1	31
404	609	3	1	31

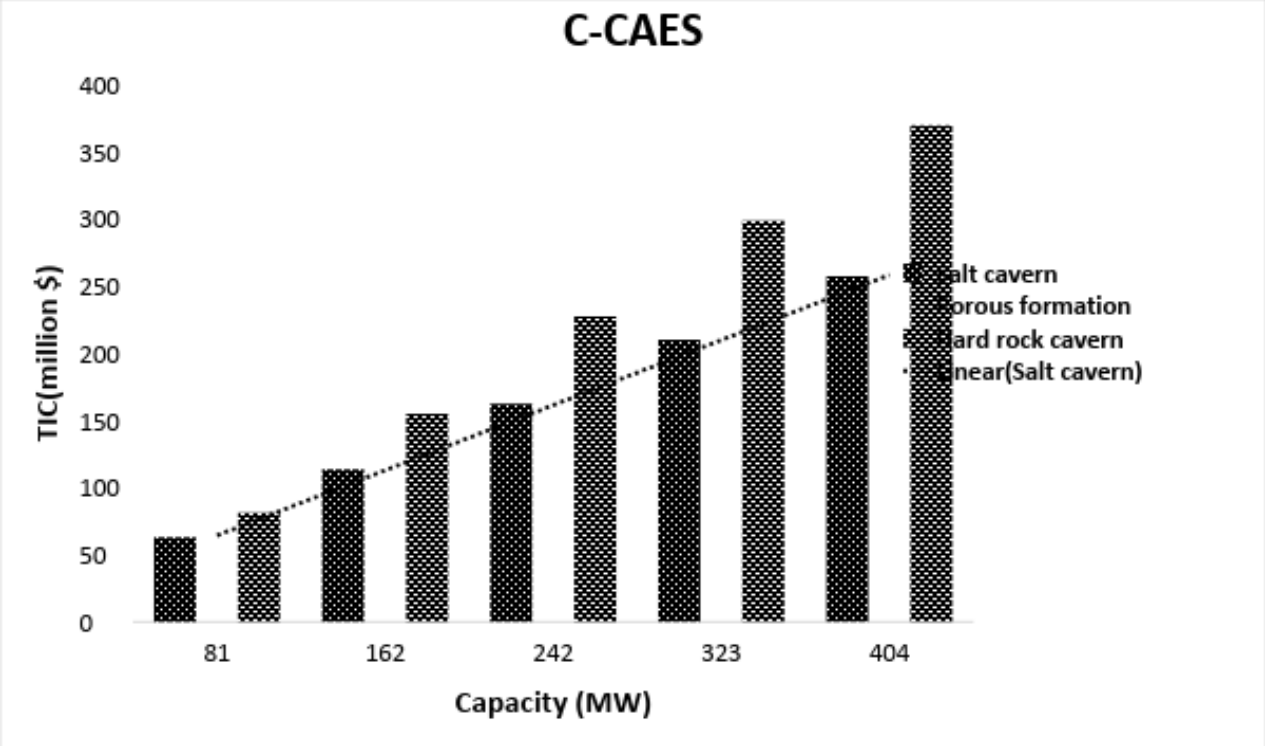

Figure 6: Total investment costs for conventional compressed air energy storage

Table 10: Power and energy cost variations with plant capacity for adiabatic compressed air energy storage

Plant Capacity (MW)	Power cost ($/kW)	Energy cost ($/kWh)		
		Salt cavern	Porous formation	Hard rock cavern
60	2228	11	4	50

119	2060	7	2	51
179	1976	5	1	51
239	1923	5	1	51
298	1884	4	1	51

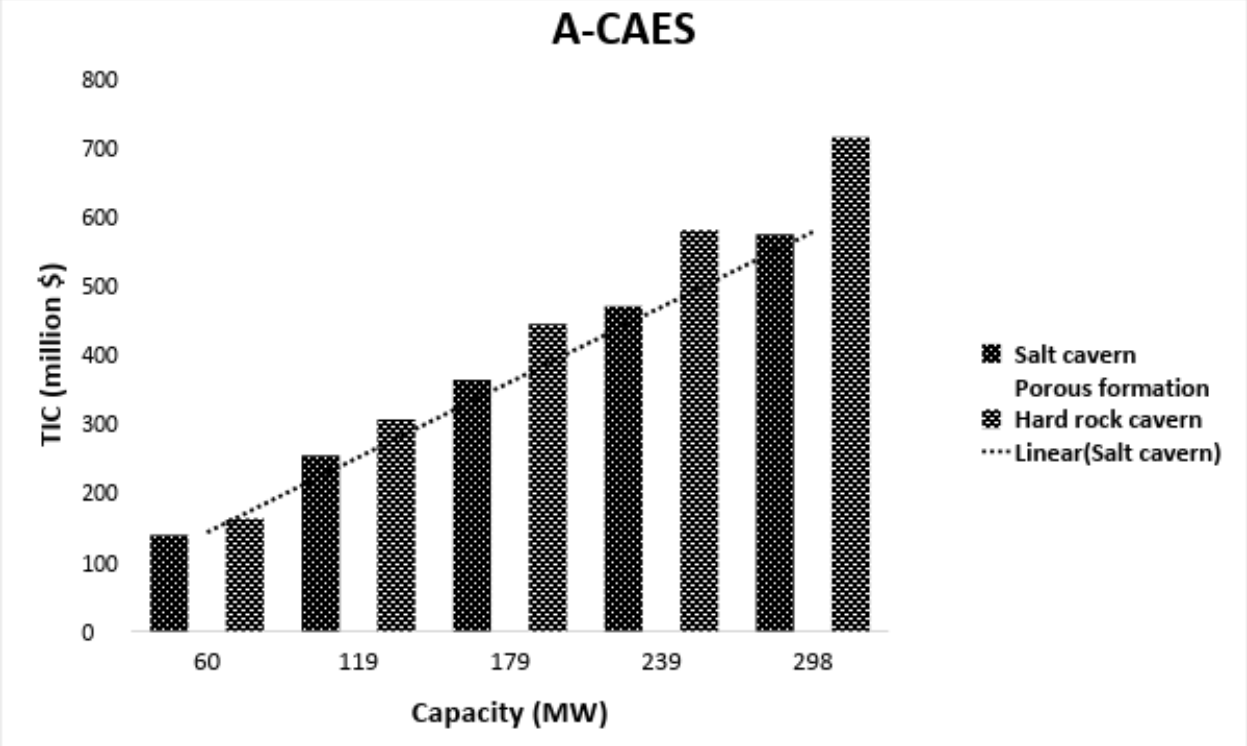

Figure 7: Total investment costs for adiabatic compressed air energy storage

The investment cost ranges are lowest for C-CAES, followed by PHS and then A-CAES. As the plant size increases, the capital cost per unit capacity decreases, showing the economy of scale benefits. The scale factor established a strong economy of scale for PHS. The energy cost for CAES is lowest for the porous formation, followed by the salt cavern. The hard rock formation is expensive to develop compared to other types of storage. As there are fewer elements involved in the construction of a porous formation, the cost is less. The above-surface air storage in pipes is currently being researched, but it is expensive and can be as high as $120 per kWh, according to Shoenung and Eyer [20].

5.1.4. Annual life cycle cost

The annual life cycle cost for PHS is shown in Figure 8. The ALCC is the indicator of annual loan repayments to cover the lifecycle costs of storage systems. Figure 8 includes the

contributing components of the ALCC. The ALCC for PHS with two-reservoir can be from $235 to $400 per kW-year and with one reservoir from $220 to $375 per kW-year. The ALCC is lower for a single reservoir as less investment is required as less capital cost is involved for one reservoir. The main component of the ALCC is the capital cost; it is more than 60% of the costs.

The ALCCs for C-CAES and A-CAES are presented in Figure 9 and 10, respectively. For C-CAES, the ALCC is from $215 to $265 per kW-year and for A-CAES, from $345 to $480 per kW-year. The major contributor for C-CAES is the annual fuel cost (electricity and natural gas) and for A-CAES is capital cost. The ALCC is highest for a hard rock formation, followed by a salt cavern; it is lowest for a porous formation. The investment cost is highest to build a hard rock cavern, followed by a salt cavern and a porous formation. The ALCC decreases with increases in a storage plant's power capacity for all storage plants because of economies of scale.

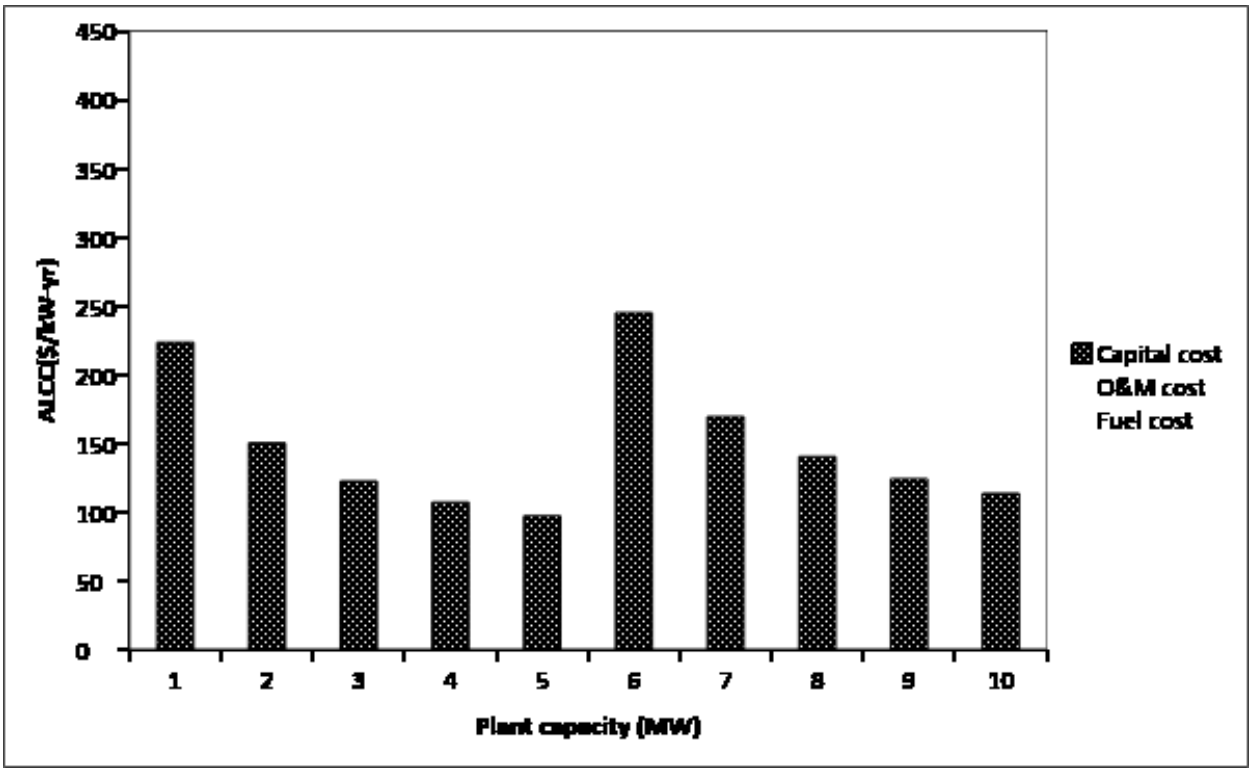

Figure 8: Annual life cycle cost for pumped hydro storage

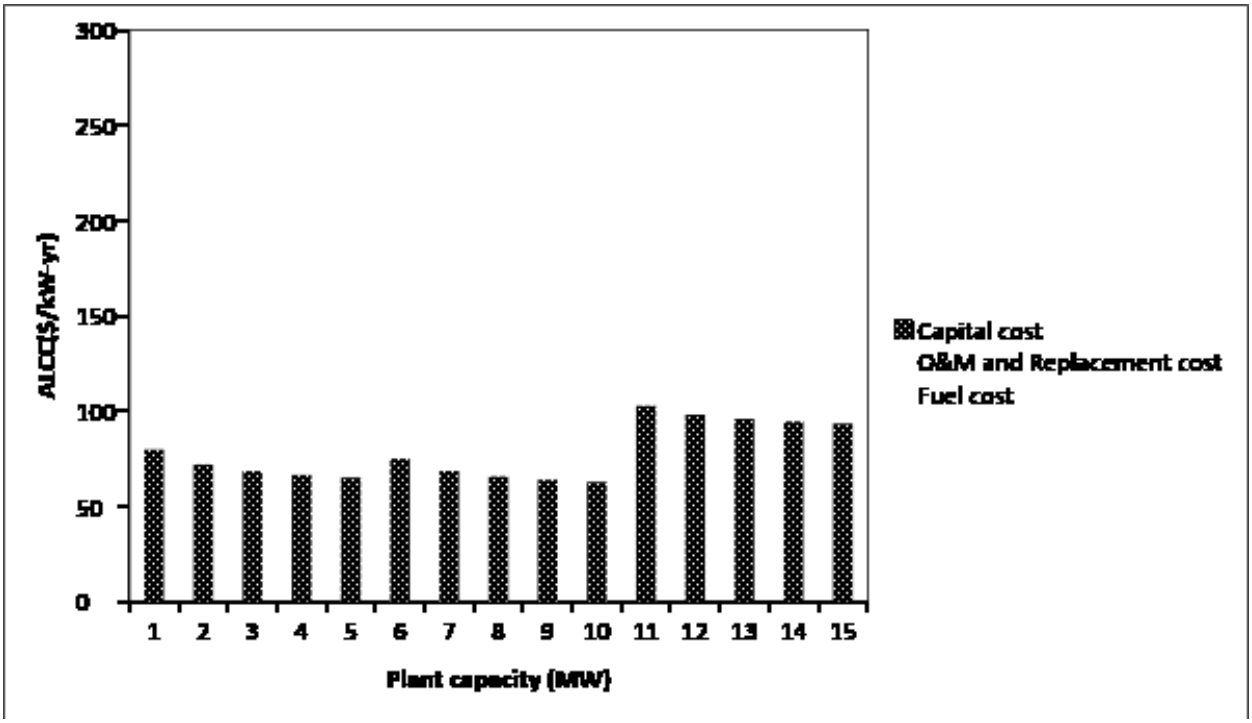

Figure 9: Annual life cycle cost for conventional compressed air energy storage

Figure 10: Annual life cycle cost for adiabatic compressed air energy storage

5.1.5. Levelised cost of electricity

The variations in the levelised cost of electricity with plant capacity for PHS are shown in Figure 11. The LCOE is from $69 to $114 MWh for the single reservoir scenario and from $73 to $121 per MWh for the two-reservoir scenario. The LCOE decreases with an increase in plant power capacity due to economies of scale, as shown in the figure. The unit capital cost decreases with an increase in plant capacity; thus, the LCOE is lower for higher capacities. The average on-peak electricity price in Alberta is $77.84 per MWh. The LCOE for a plant with a higher power capacity, such as 392 or 490 MW, is less than Alberta's on-peak electricity price. For lower plant capacities, the LCOE is more than the average on-peak price in Alberta.

The LCOE for C-CAES and A-CAES is presented in Figure 12 and 13. The LCOE for C-CAES is $58 to $64 per MWh for the salt cavern, $58 to $63 per MWh for the porous formation, and $65 to $70 per MWh for the hard rock cavern. The LCOE for A-CAES is $97 to $112 per MWh for the salt cavern, $96 to $110 per MWh for the porous formation, and $108 to $121 per MWh for the hard rock cavern. The LCOEs for the salt cavern and porous formation are similar. The hard rock cavern scenario has a higher LCOE than the other scenarios because of the higher

storage cost component. The LCOE for the C-CAES for all three storage types is lower than the average on-peak electricity price in Alberta. The LCOE for A-CAES for all storage types is higher than the average on-peak electricity price in Alberta.

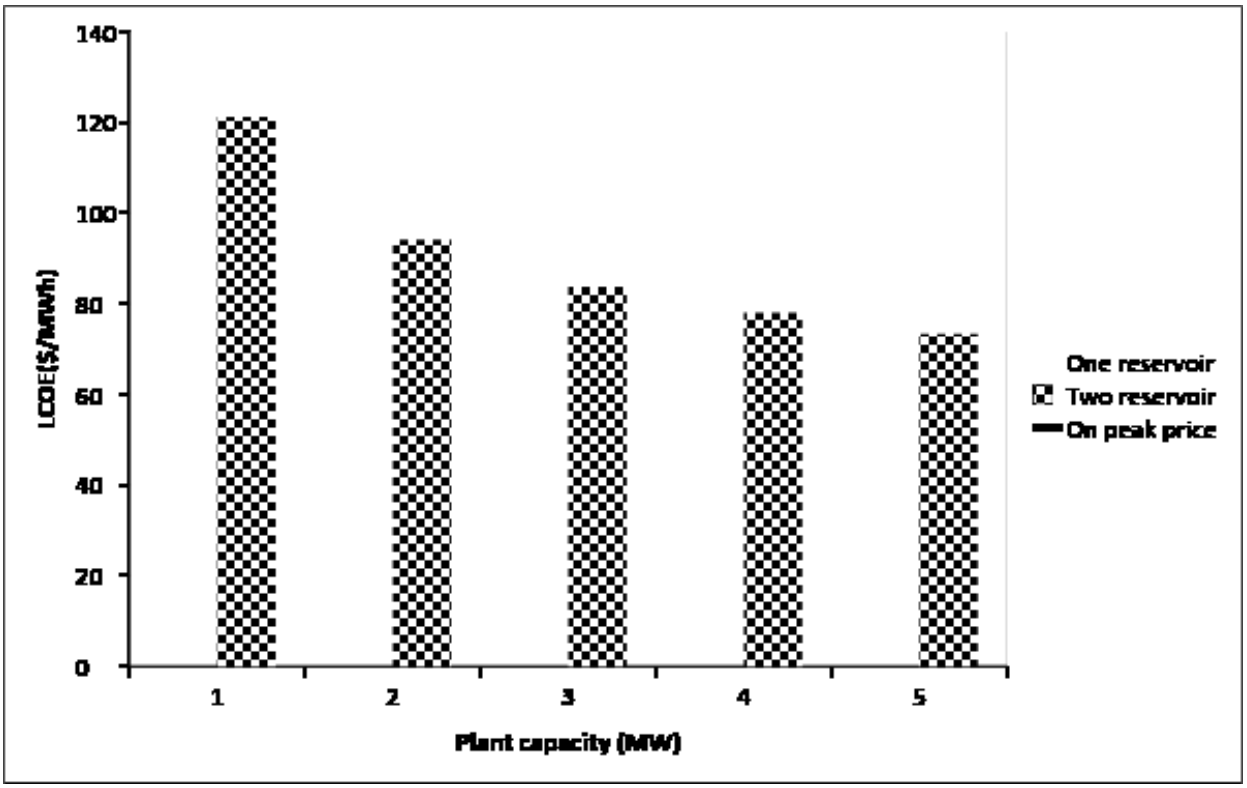

Figure 11: Variations of the levelised cost of electricity with plant capacity for pumped hydro storage

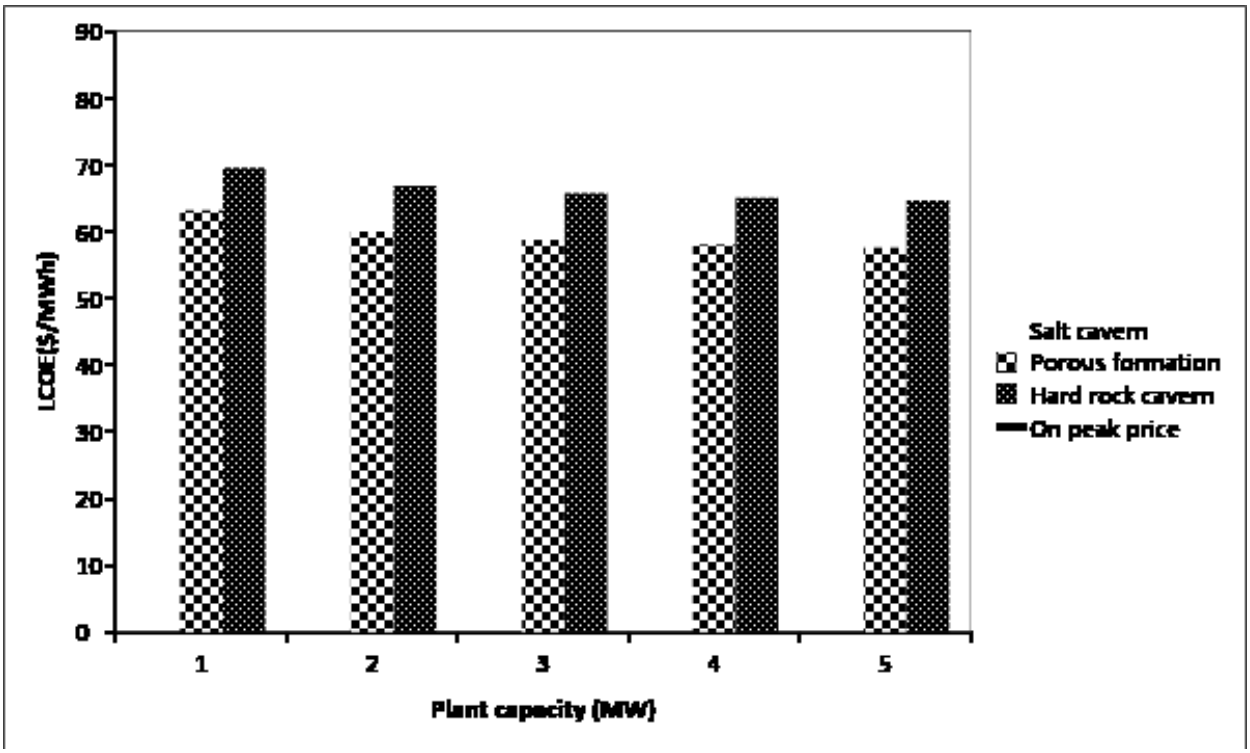

Figure 12: Variations of levelised cost of electricity with plant capacity for conventional compressed air energy storage

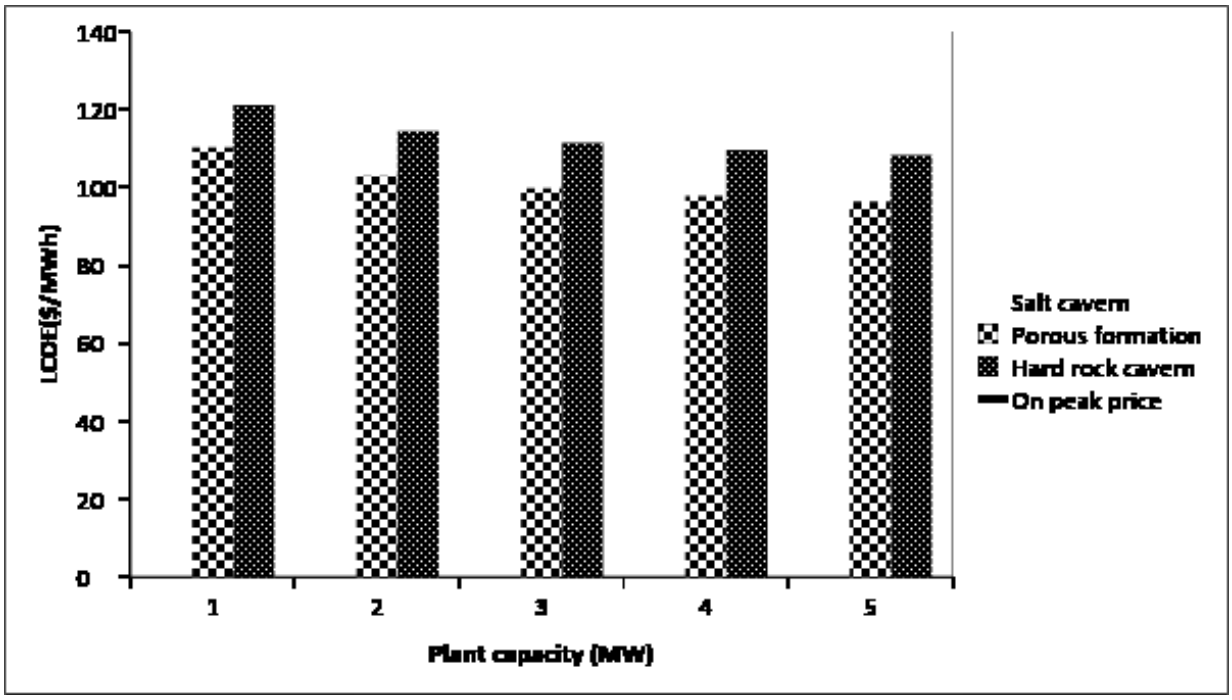

Figure 13: Variations of levelised cost of electricity with plant capacity for adiabatic compressed air energy storage

5.1.6. Levelised Cost of Storage (LCOS)

The variations in levelised cost of storage with plant capacity for PHS are presented in Figure 14. The LCOS is as low as $34 per MWh for a plant capacity of 491 MW and as high as $86 per MWh for a plant capacity of 98 MW. Again, the variation is due to decreases in unit capital cost with increases in plant capacity. As the unit capital cost is lower for higher capacities, the LCOS is less. The LCOS decreases with an increase in plant power capacity through economies of scale. The LCOS is from $34 to $79 per MWh for the one reservoir scenario and $39 to $86 per MWh for the two-reservoir scenario. The results of the LCOS were compared with the differences between on-peak and off-peak electricity prices in Alberta, otherwise known as the opportunity cost. The LCOS for PHS is lower than the opportunity cost for plant capacities of 294 MW, 392 MW, and 491 MW.

The LCOS for C-CAES and A-CAES is presented in Figure 15 and Figure 16, respectively. The LCOE for C-CAES ranges from $19 to $25 per MWh for the salt cavern, $19 to $24 per MWh for the porous formation, and $25 to $31 per MWh for the hard rock cavern. The LCOE for A-CAES ranges from $57 to $72 per MWh for the salt cavern, $56 to $70 per MWh for the porous formation, and $68 to $81 per MWh for the hard rock cavern. The LCOS for C-CAES is lower

than the opportunity cost for all storage types and thus favorable. The LCOS for A-CAES is higher than the opportunity cost and thus not promising at all.

The greater the difference in unit capital cost the wider spread the LCOS. Thus, the variation in LCOS is greater for PHS than for CAES.

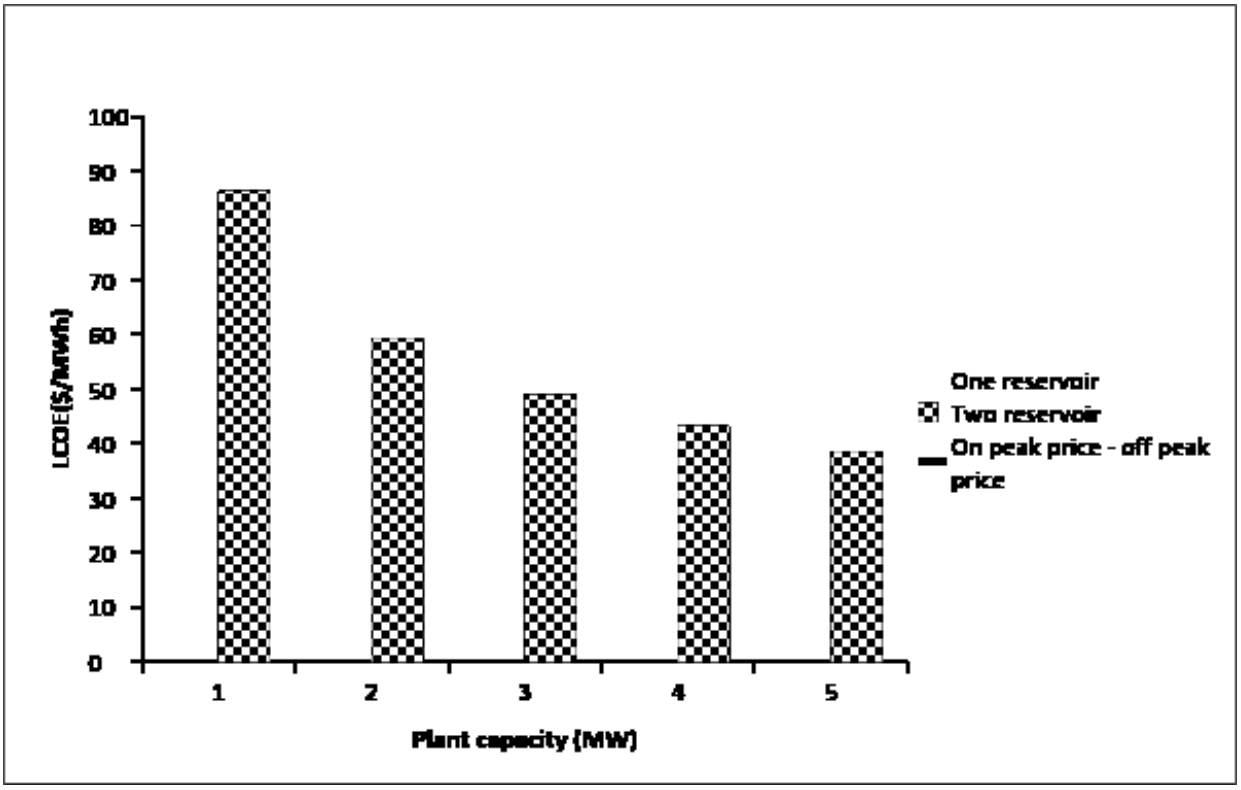

Figure 14: Variations of levelised cost of storage with plant capacity for pumped hydro storage

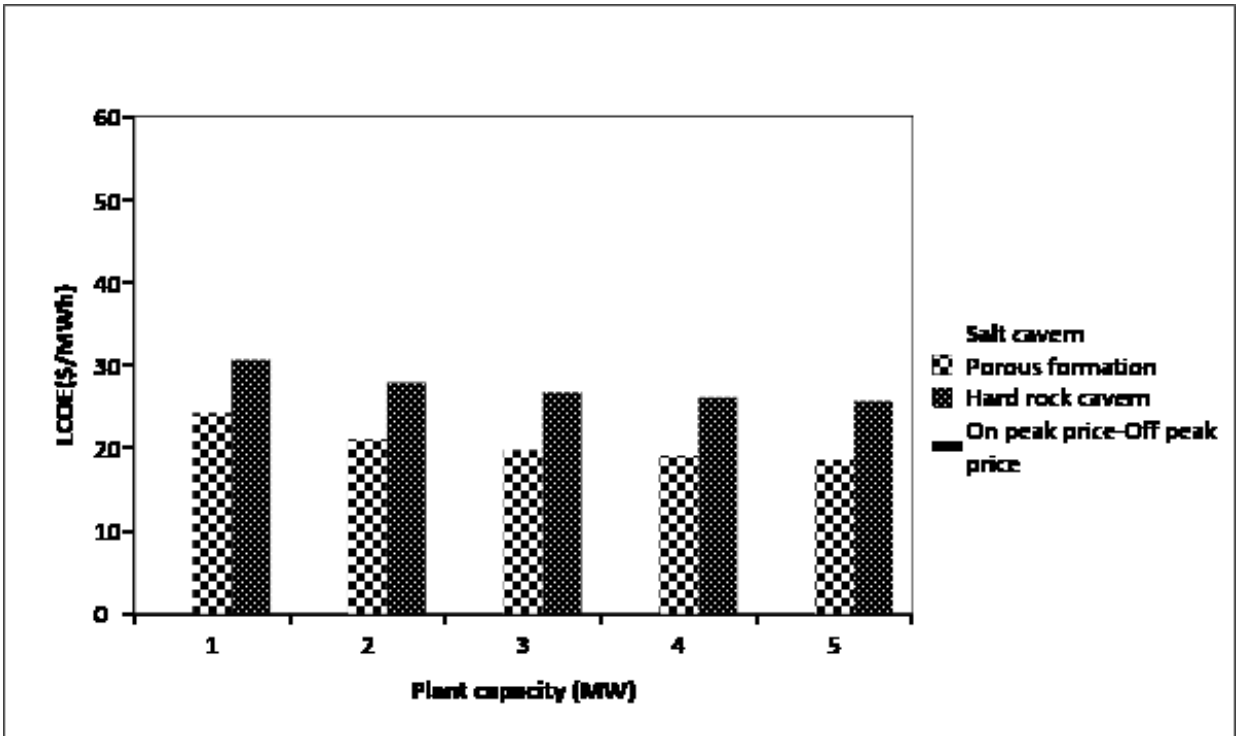

Figure 15: Variations of levelised cost of storage with plant capacity for conventional compressed air energy storage

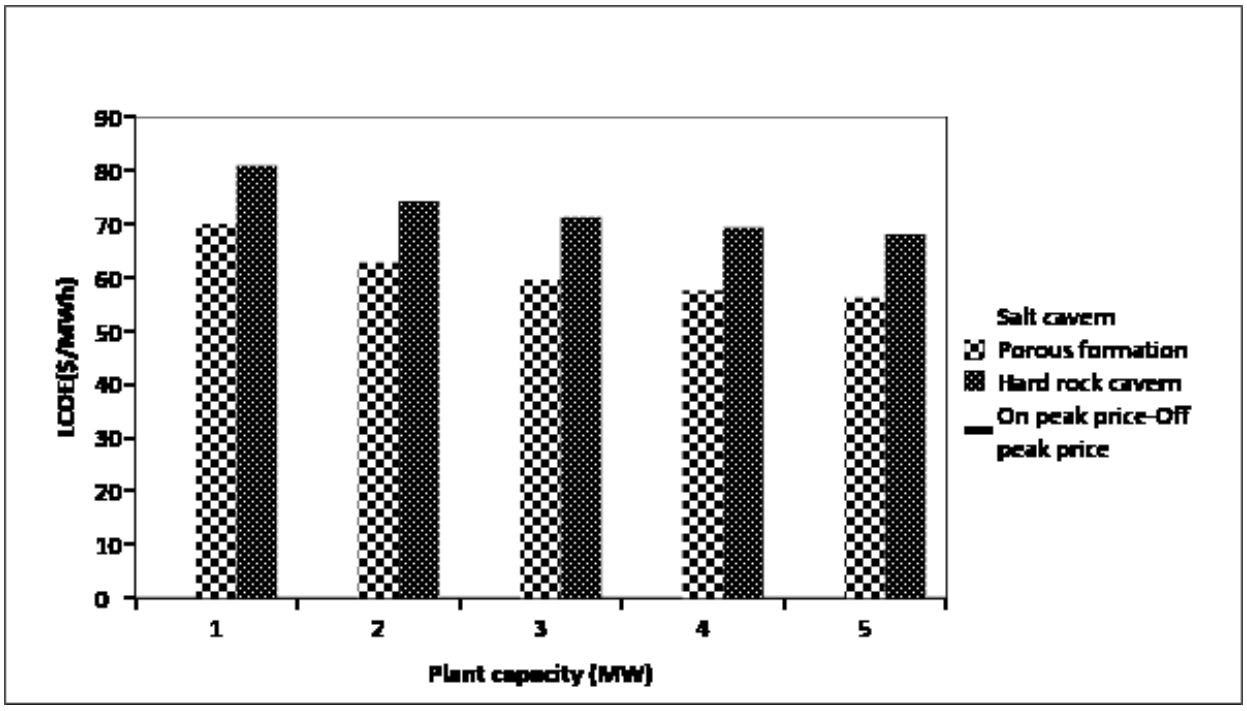

Figure 16: Variations of levelised cost of storage with plant capacity for adiabatic compressed air energy storage

5.2. Sensitivity Analysis

A sensitivity analysis was conducted to determine the influence of key process and cost parameters on the cost of electricity produced from the storage plant. The parameters selected are in one of three categories: technical, cost, and economic parameters. The technical parameters selected for PHS are head, water flow rate, hours of operation, and pump turbine efficiency. The technical parameters selected for CAES are turbine efficiency, hours of operation, airflow rate, and turbine inlet temperature. As equipment costs are derived from the literature, it is important to study their effect on the LCOE to build confidence in cost numbers. Cost parameters include the TIC, O&M cost, and high-cost equipment. Based on the classification provided by the Association for the Advancement of Cost Estimating International, the estimated costs for technologies are class 4 preliminary estimates and have an accuracy range of ±30% [62]. This range was used in the sensitivity analysis. In addition, economic parameters such as fuel cost, electricity cost, inflation, and discount rate were included to study their impact on the LCOE.

The PHS base case has a capacity of 294 MW with two-reservoir and an LCOE of $83.76 per MWh. The sensitivity analysis results for PHS are presented in Figure 17. The LCOE is most

sensitive to the efficiency of the pump turbine. An increase in pump turbine efficiency reduces system energy losses, thus increasing the electricity output from the system. The capital cost of the pump turbine increases with an increase in efficiency, though the overall impact on the entire system is relatively insignificant. As there is more energy output from the PHS plant, the LCOE decreases. A 5% increase in pump turbine efficiency will decrease the LCOE by 4.8%. Other highly sensitive parameters for PHS are hours of operation and discount rate.

The C-CAES base case has a capacity of 242 MW with salt cavern storage and an LCOE of $59.46 per MWh. The results of the sensitivity analysis for C-CAES are presented in Figure 18. The LCOE is most sensitive to the inlet temperature of the second turbine. If the inlet temperature of the second turbine increases by 5%, the LCOE goes down by 1.9%. The turbine inlet temperature is directly proportional to the energy output from the CAES plant, thus leading to a decrease in the LCOE. Other highly sensitive parameters are hours of operation and the TIC.

The A-CAES base case has a capacity of 179 MW with salt cavern storage and an LCOE of $100.78 per MWh. The results of the sensitivity analysis for A-CAES are presented in Figure 19. For A-CAES, the most sensitive parameter is air flow rate. The plant capacity is dependent on air flow rate and, a decrease in air flow rate results in a smaller plant size. Further, due to economies of scale, the LCOE increases. A 5% decrease in air flow rate increases the LCOE by 3.8%. Other sensitive parameters are air inlet temperature and the TIC.

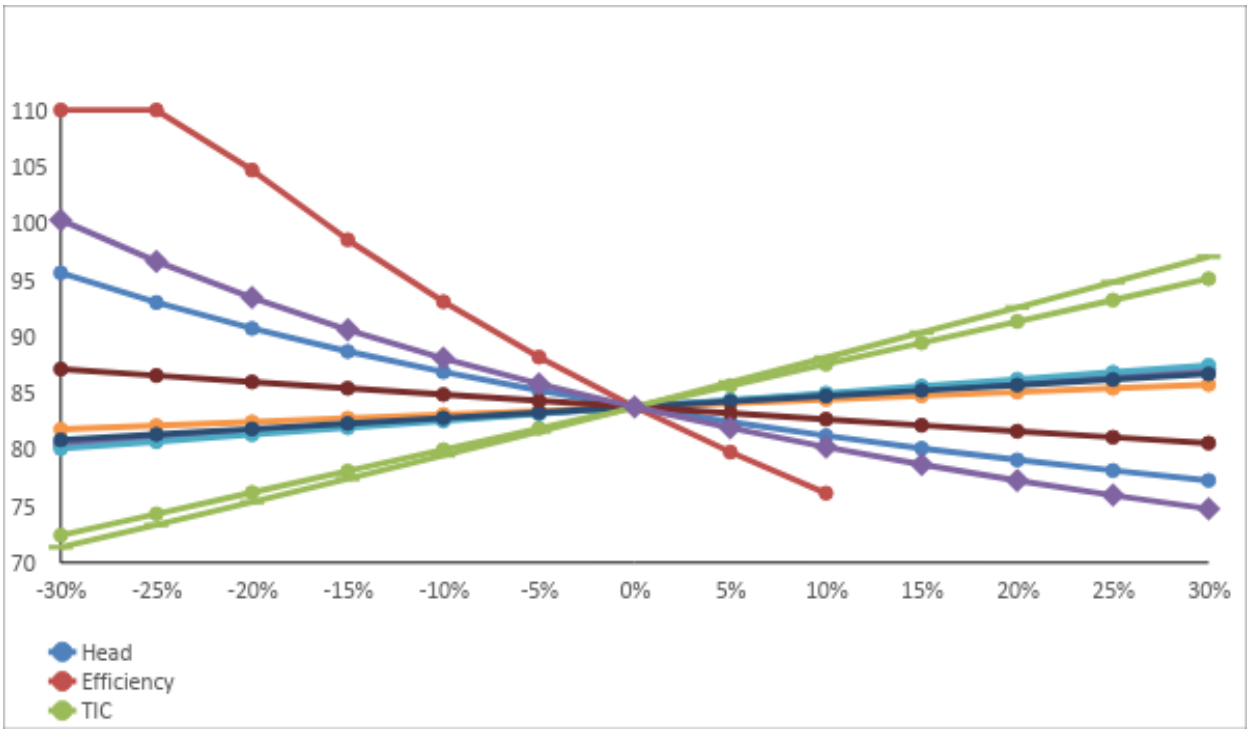

Figure 17: Effect of variations of different parameters on the levelised cost of electricity for pumped hydro storage

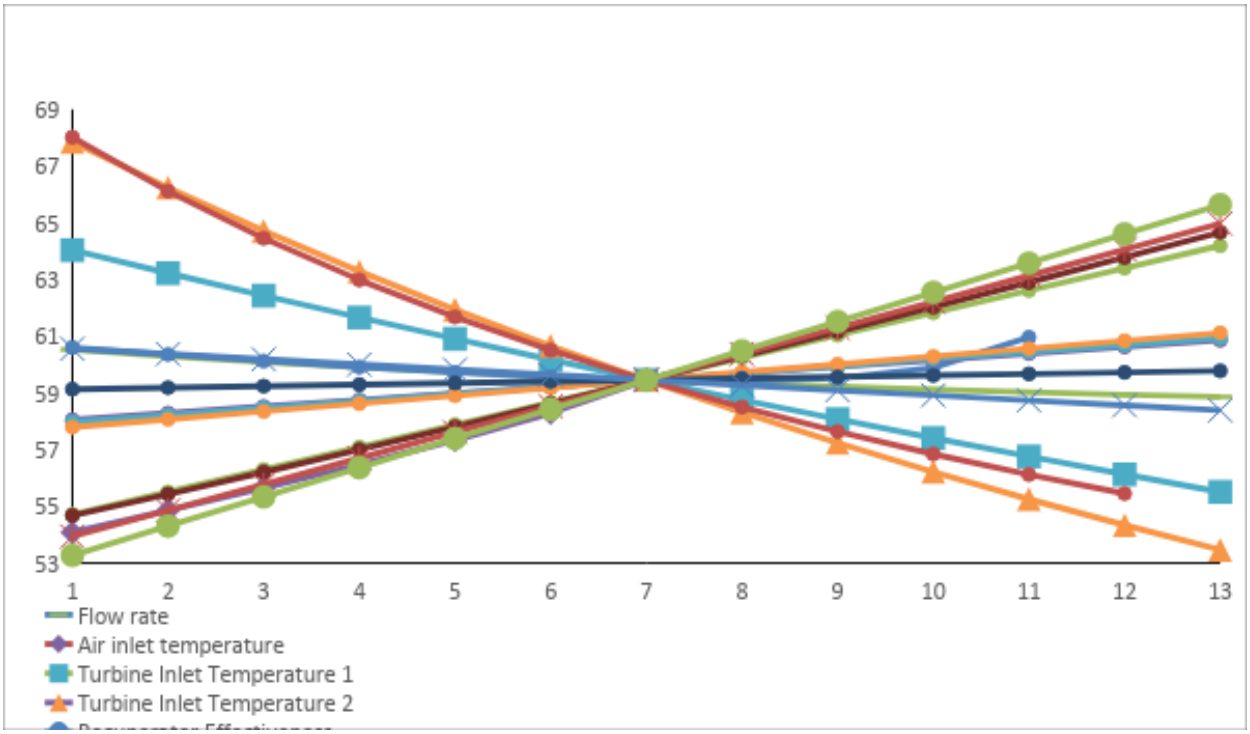

Figure 18: Effect of variations of different parameters on the levelised cost of electricity for conventional compressed air energy storage

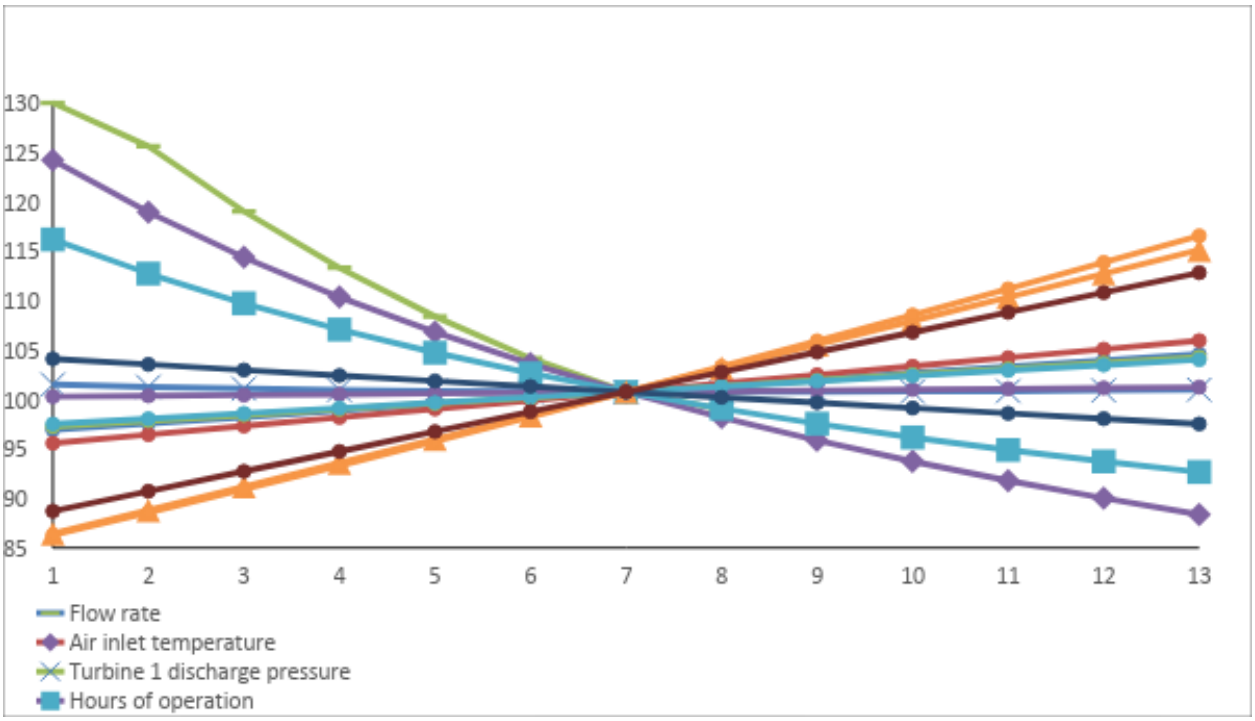

Figure 19: Effect of variations of different parameters on the levelised cost of electricity for adiabatic compressed air energy storage

5.3. Uncertainty analysis

An uncertainty analysis was performed to evaluate the effect of simultaneous change in input variable on final output. An uncertainty analysis was also conducted to understand the risks and impacts of uncertainties in input process parameters on the LCOE. The Monte Carlo simulation technique and ModelRisk software were used to perform the analysis. A random value was selected from the range of input variables that have an impact on the final output. The process is iterated a number to times, taking random input values every time to obtain a range of values for the final output. The Monte Carlo simulation was performed for the PHS, C-CAES, and A-CAES base cases by identifying the input parameters and quantifying the uncertainty in the LCOE with 50,000 iterations each. The various input variables selected for uncertainty analysis and their ranges are reported in Table 11. The results of this analysis are presented in Figure 20. The mean LCOE for PHS is $96.82 per MWh and for C-CAES and A-CAES is $57.87 and $104.48 per MWh, respectively.

Table 11: Uncertainty analysis parameters

Parameter	Minimu	Base	Maximum	Unit	Referenc

		m value	value	value		e
PHS						
	Head	100	500	1200	m	[30, 31]
	efficiency (pump)	0.8	0.9	0.95		[30, 31]
	efficiency (Turbine)	0.8	0.9	0.95		[30, 31]
	Hours of operation	6	8	10	h	[30, 31]
	Flow rate (m^3/s)	20	60	120	m^3/s	[30, 31]
	Velocity of flow	4	5	10	m/s	[30, 31]
C-CAES						
	Flow rate	285	300	315	m^3/s	
	Air Inlet temperature	273.15	288.15	298.15	K	
	Turbine 1 temperature	810.15	823.15	823.15	K	[37, 44]
	Turbine 2 temperature	1073.15	1073.15	1144.15	K	[37, 44]
	Electricity Cost	21.29	28.18	36.55	$/MWh	[60]
	NG cost	0.125	0.23	0.26	$/kg	
A-CAES						
	Flow rate	285	300	315	m^3/s	
	Air Inlet temperature	273.15	288.15	298.15	K	
	Electricity Cost	21.29	28.18	36.55	$/MWh	[60]

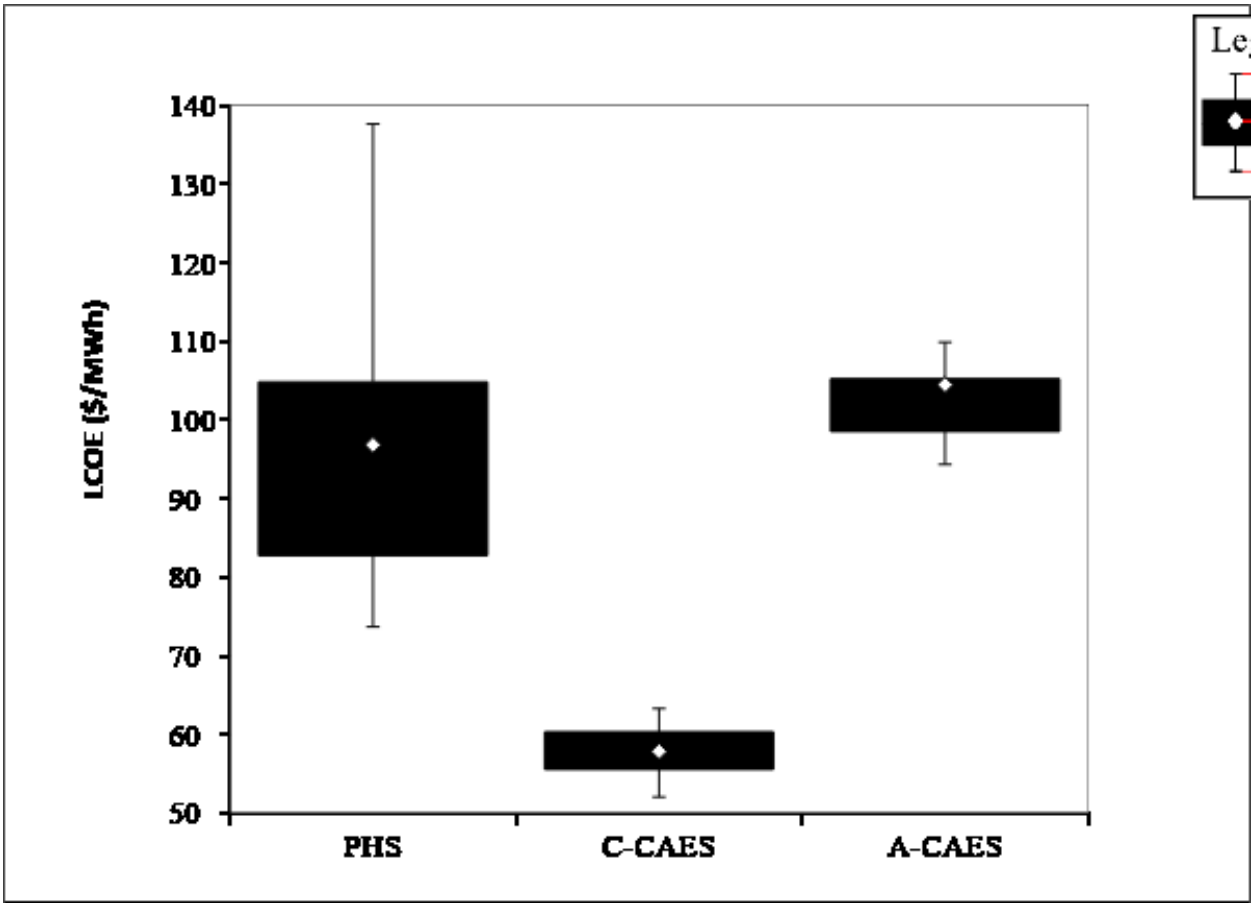

Figure 20: Results of uncertainty analysis

In this study, the LCOEs for PHS and CAES are $69-121 per MWh and $58-70 per MWh, respectively. These results were compared with the values reported by Zakeri et al. [25] and the DOE/EPRI report [22]. The LCOEs for PHS and CAES reported by Zakeri et al. [25] are in the range of $125-150 per MWh and $130-160 per MWh, respectively, while the values reported by DOE/EPRI [22] are $150-220 per MWh for PHS and $120-210 per MWh for CAES. The values presented by Zakeri et al. are higher due to the high cost of the storage medium and the location factor. The price of electricity input to the system is strongly influenced by jurisdiction and thus is higher in this case. In this study, by considering a salt cavern as a storage medium, capital cost is significantly lowered, i.e., by $2-5/kWh. On the other hand, it is difficult to compare the values reported by DOE/EPRI [22] because the details of the plant components and system boundaries were not stated.

Conclusion

The objective of the study was to develop data-intensive comprehensive cost models, calculate lifecycle costs for PHS and CAES, and evaluate the economic feasibility of ESS. To that end, equipment parameters and costs for PHS and CAES were estimated using a detailed bottom-up cost calculation methodology. A techno-economic model was developed to investigate the power output of the storage plant. Five scenarios for each EES technology considered were modeled encompassing different plant storage capacities ranging from 98 to 491 MW, 81 MW to 404 MW, and 60 to 298 MW for PHS, C-CAES, and A-CAES, respectively. The TIC of these scenarios was calculated using the equipment cost relation and compared. The TIC decreases with increases in plant capacity due to economies of scale. The developed scale factors for PHS, C-CAES, and A-CAES are 0.5, 0.9, and 0.91, respectively. The scale factors show that the additional unit investment cost falls sharply with increases in capacity for PHS and thus it is beneficial to build plants in higher capacities. The unit output capital cost is lowest for C-CAES, followed by PHS and then A-CAES.

For CAES, three storage types were considered. The cost is lowest for a porous formation, slightly higher for a salt cavern, and highest for a hard rock formation. The LCOEs for the PHS, C-CAES, and A-CAES base cases are $84, $59, and $101 per MWh, respectively. The LCOE decreases with an increase in plant capacity because of economies of scale. For Alberta's electricity market, C-CAES integrated with any storage type and capacity is a sound financial investment. PHS yields profits for plant capacities greater than 294 MW. A-CAES is not feasible for energy arbitrage due to a higher LCOE.

A sensitivity analysis showed that the pump turbine efficiency, inlet temperature to second turbine, and air flow rate are the most sensitive parameters for PHS, C-CAES, and A-CAES, respectively.

To provide more robustness to the developed model and mitigate risk, an uncertainty analysis was performed and yielded mean LCOEs of $96.82 per MWh, $57.87 per MWh, and $104.48 per MWh for PHS, C-CAES, and A-CAES, respectively.

The results of this techno-economic study provide insight on the cost competitiveness of PHS and CAES.

Acknowledgement

The authors thank the NSERC Energy Storage Technology (NEST) Network (RYERU NSERC 468468 Kumar) and the University of Alberta (UOFAB VPRGRF NEST KUMAR) for the financial

support provided to carry out this research. The authors are thankful to Astrid Blodgett for editing this paper.

References

1. Kousksou, T., et al., *Energy storage: Applications and challenges.* Solar Energy Materials and Solar Cells, 2014. **120, Part A**: p. 59-80.
2. *World Energy Outlook Special Report 2016: Energy and Air Pollution*. 2016. p. 266.
3. Poullikkas, A., *Implementation of distributed generation technologies in isolated power systems.* Renewable and Sustainable Energy Reviews, 2007. **11**(1): p. 30-56.
4. Fisher, A.C., *Energy and environment in the long term.* Energy Policy, 1989. **17**(2): p. 84-87.
5. Rogelj, J., et al., *Paris Agreement climate proposals need a boost to keep warming well below 2 C.* Nature, 2016. **534**(7609): p. 631-639.
6. Aneke, M. and M. Wang, *Energy storage technologies and real life applications – A state of the art review.* Applied Energy, 2016. **179**: p. 350-377.
7. Luo, X., et al., *Overview of current development in electrical energy storage technologies and the application potential in power system operation.* Applied Energy, 2015. **137**: p. 511-536.
8. Martinot, E., *Renewables 2015: Global status report.* REN21 Renewable Energy Policy Network/Worldwatch Institute, 2015: p. 251.
9. Hadjipaschalis, I., A. Poullikkas, and V. Efthimiou, *Overview of current and future energy storage technologies for electric power applications.* Renewable and Sustainable Energy Reviews, 2009. **13**(6–7): p. 1513-1522.
10. Decourt, B.D., Romain; , *Electricity Storage*, in *Leading the energy transition*. 2013.
11. Chen, H., et al., *Progress in electrical energy storage system: A critical review.* Progress in Natural Science, 2009. **19**(3): p. 291-312.
12. Beaudin, M., et al., *Energy storage for mitigating the variability of renewable electricity sources: An updated review.* Energy for Sustainable Development, 2010. **14**(4): p. 302-314.
13. Ferreira, H.L., et al., *Characterisation of electrical energy storage technologies.* Energy, 2013. **53**: p. 288-298.
14. Cavallo, A.J., *Energy storage technologies for utility scale intermittent renewable energy systems.* Journal of solar energy engineering, 2001. **123**(4): p. 387-389.
15. Ibrahim, H., A. Ilinca, and J. Perron, *Energy storage systems—Characteristics and comparisons.* Renewable and Sustainable Energy Reviews, 2008. **12**(5): p. 1221-1250.
16. Connolly, D., *A review of energy storage technologies: For the integration of fluctuating renewable energy*. 2010.
17. Palizban, O. and K. Kauhaniemi, *Energy storage systems in modern grids—Matrix of technologies and applications.* Journal of Energy Storage, 2016. **6**: p. 248-259.
18. Mahlia, T.M.I., et al., *A review of available methods and development on energy storage; technology update.* Renewable and Sustainable Energy Reviews, 2014. **33**: p. 532-545.
19. Schoenung, S.M. and W.V. Hassenzahl, *Long-vs. short-term energy storage technologies analysis. a life-cycle cost study. a study for the doe energy storage systems program.* Sandia National Laboratories, 2003.
20. Schoenung, S.M. and J. Eyer, *Benefit/cost framework for evaluating modular energy storage.* SAND2008-0978, 2008.

21. Schoenung, S., *Energy Storage Systems Cost Update* 2011.
22. Akhil, A.A., et al., *DOE/EPRI 2013 electricity storage handbook in collaboration with NRECA*. 2013: Sandia National Laboratories Albuquerque, NM.
23. Viswanathan, V., et al., *National Assessment of Energy Storage for Grid Balancing and Arbitrage, Phase II, Volume 2: Cost and Performance Characterization.* Report PNNL-21388, Pacific Northwest National Laboratory, Richland, WA, 2013.
24. Bozzolani, E., *Techno-economic analysis of compressed air energy storage systems.* 2010.
25. Zakeri, B. and S. Syri, *Electrical energy storage systems: A comparative life cycle cost analysis.* Renewable and Sustainable Energy Reviews, 2015. **42**: p. 569-596.
26. Locatelli, G., E. Palerma, and M. Mancini, *Assessing the economics of large Energy Storage Plants with an optimisation methodology.* Energy, 2015. **83**: p. 15-28.
27. Denholm, P. and G.L. Kulcinski, *Life cycle energy requirements and greenhouse gas emissions from large scale energy storage systems.* Energy Conversion and Management, 2004. **45**(13–14): p. 2153-2172.
28. *Technology Roadmap Energy storage*. 2014: France.
29. Rastler, D., *Electricity energy storage technology options: a white paper primer on applications, costs and benefits*. 2010: Electric Power Research Institute.
30. American Society of Civil, E., *Compendium of pumped storage plants in the United States*. 1993, New York, NY: The Society. 744 p.
31. Carson, J., et al., *Operation and maintenance experiences of pumped-storage plants*. 1991, Morrison-Knudsen Engineers, Inc., San Francisco, CA (USA); Electric Power Research Inst., Palo Alto, CA (USA).
32. Stelzer, R.S. and R.N. Walters, *Estimating reversible pump-turbine characteristics*. 1977, Bureau of Reclamation, Denver, CO (USA). Engineering and Research Center.
33. Korakianitis, T. and D.G. Wilson, *Models for Predicting the Performance of Brayton-Cycle Engines.* Journal of Engineering for Gas Turbines and Power, 1994. **116**(2): p. 381-388.
34. Cohen, H., et al., *Gas turbine theory.* 1987.
35. Borgnakke, C. and R.E. Sonntag, *Fundamentals of thermodynamics*. 2009: Wiley.
36. Cengel, Y.A. and M.A. Boles, *Thermodynamics: an engineering approach.* Sea, 1994. **1000**: p. 8862.
37. Pollak, R., *History of First US Compressed-Air Energy Storage (CAES) Plant (110 MW 26h) Volume 2: Construction.* Electric Power Research Institute (EPRI), 1994.
38. Kays, W.M., R.K. Jain, and S. Sabherwal, *The effectiveness of a counter-flow heat exchanger with cross-flow headers.* International Journal of Heat and Mass Transfer, 1968. **11**(4): p. 772-774.
39. Kyle, B.G., *Chemical and process thermodynamics.* 1984.
40. Moore, W.J., *Basic physical chemistry*. 1983: Prentice Hall.
41. Walsh, P.P. and P. Fletcher, *Gas turbine performance*. 2004: John Wiley & Sons.
42. *Overall Heat Transfer Coefficient Table Charts and Equation* 2017 [cited 2017 July 1]; Available from: http://www.engineersedge.com/thermodynamics/overall_heat_transfer-table.htm.
43. McDonald, A.G. and H. Magande, *Introduction to thermo-fluids systems design*. 2012: John Wiley & Sons.
44. Crotogino, F., et al., *More than 20 years of successful operation. Spring 2001 Meeting of the Solution Mining Research Institute*. April.
45. Kaya, D., et al., *Energy efficiency in pumps.* Energy Conversion and Management, 2008. **49**(6): p. 1662-1673.
46. *Typical overall heat transfer coefficients (U-Values)*. 2017 [cited 2017 July 2]; Available from: http://www.engineeringpage.com/technology/thermal/transfer.html.

47. Jubeh, N.M. and Y.S. Najjar, *Green solution for power generation by adoption of adiabatic CAES system.* Applied Thermal Engineering, 2012. **44**: p. 85-89.
48. Gabbrielli, R. and R. Singh, *Economic and scenario analyses of new gas turbine combined cycles with no emissions of carbon dioxide.* Journal of engineering for gas turbines and power, 2005. **127**(3): p. 531-538.
49. Turton, R., et al., *Analysis, synthesis and design of chemical processes*. 2008: Pearson Education.
50. Norge, A., *Cost base for hydropower plants* J. Slapgård, Editor. 2012: Norway.
51. Dawes, J.H. and M. Wathne, *Cost of reservoirs in Illinois*. 1968: Illinois State Water Survey.
52. *Land value trends*. 2013: Alberta. p. 6.
53. Goodson, O.J., *History of First U.S. Compressed Air Energy Storage (CAES) Plant (110-MW-26 h): Volume 1: Early CAES Development*. 1993. p. 150.
54. Miller, P.C. *Bakken has lowest average drilling and completion cost*. 2016 April 06, 2016 [cited 2017 July 2]; Available from: http://thebakken.com/articles/1515/bakken-has-lowest-average-drilling-and-completion-cost.
55. *OCCinfo: Occupations and Educational Programs* 2015 [cited 2017 July 2]; Available from: http://occinfo.alis.alberta.ca/occinfopreview/info/browse-wages.html.
56. Peters, M.S., et al., *Plant design and economics for chemical engineers*. Vol. 4. 1968: McGraw-Hill New York.
57. Zamalloa, C., et al., *The techno-economic potential of renewable energy through the anaerobic digestion of microalgae.* Bioresource Technology, 2011. **102**(2): p. 1149-1158.
58. Veatch, B., *Cost and Performance Data for Power Generation Technologies.* Cost Report, ed. BVH Company, 2012.
59. Taylor, M., *Renewable Energy Technologies: Cost Analysis Series*, in *Hydropower*. 2012. p. 144.
60. *2014 Annual Market Statistics*. 2015.
61. *Inflation*. [cited 2017 july 2]; Available from: http://www.bankofcanada.ca/core-functions/monetary-policy/inflation/.
62. Towler, G. and R. Sinnott, *Chapter 7 - Capital Cost Estimating*, in *Chemical Engineering Design (Second Edition)*. 2013, Butterworth-Heinemann: Boston. p. 307-354.